

Cobar-style polymetallic Au-Cu-Ag-Pb-Zn deposits

Kenneth C. Lawrie[1] & Mark C. Hinman[2]

James Cook University of North Queensland, Townsville, Queensland 4811, Australia. [1]current address Australian Geological Survey Organisation, GPO Box 378, Canberra, ACT 2601, Australia. [2]current address GeoSOLUTIONS, 43 Gerler St, Bardon, Queensland 4065, Australia.

EXPLORATION MODEL

Examples

Elura, Peak, CSA, Great Cobar, New Cobar, Chesney, New Occidental, McKinnons (Australia).

Target

- Major deposit types include: Au–Cu, Cu–minor Au, Au–Cu–Pb–Zn, Cu–Zn–Pb–Ag, and Ag–Pb–Zn–(Cu).
- Deposit size varies markedly: 30 Mt @ 14% Pb + Zn + 139 g/t Ag (Elura); 17 Mt @ 1.3% Cu + 4.5% Pb + Zn (CSA); 4.6 Mt @ 8.8 g/t Au , 3% Cu + Pb + Zn (Peak).
- Deposits comprise multiple ore lenses; metal ratios vary significantly between adjacent lodes, with vertical and lateral zonation within individual lodes.
- Cu–Au orebodies are generally much lower in total sulphide than Ag–Pb–Zn lodes.

Mining and treatment

- Vertical continuity of orebodies and grades facilitates underground mining by long-hole open stoping.
- Metal recoveries often hindered by complex polymetallic mineralogy and high pyrite content.
- Very fine grain size requires micro-milling.
- Au association with base-metal sulphides in lodes with variable grades and metal ratios requires flexible milling and complex metallurgical processing.
- Ag recoveries reduced, owing to association with sulphosalts in primary ore at Elura.
- High orebody delineation costs associated with more vein-like lodes and lateral and vertical metal zonation.
- Variable, high Fe content in sphalerite can be a problem.
- Smelter penalties in some orebodies, e.g. As content in Elura concentrates and Pb in Peak Cu concentrates.
- Hardness of gangue silicification is a factor in crushing.

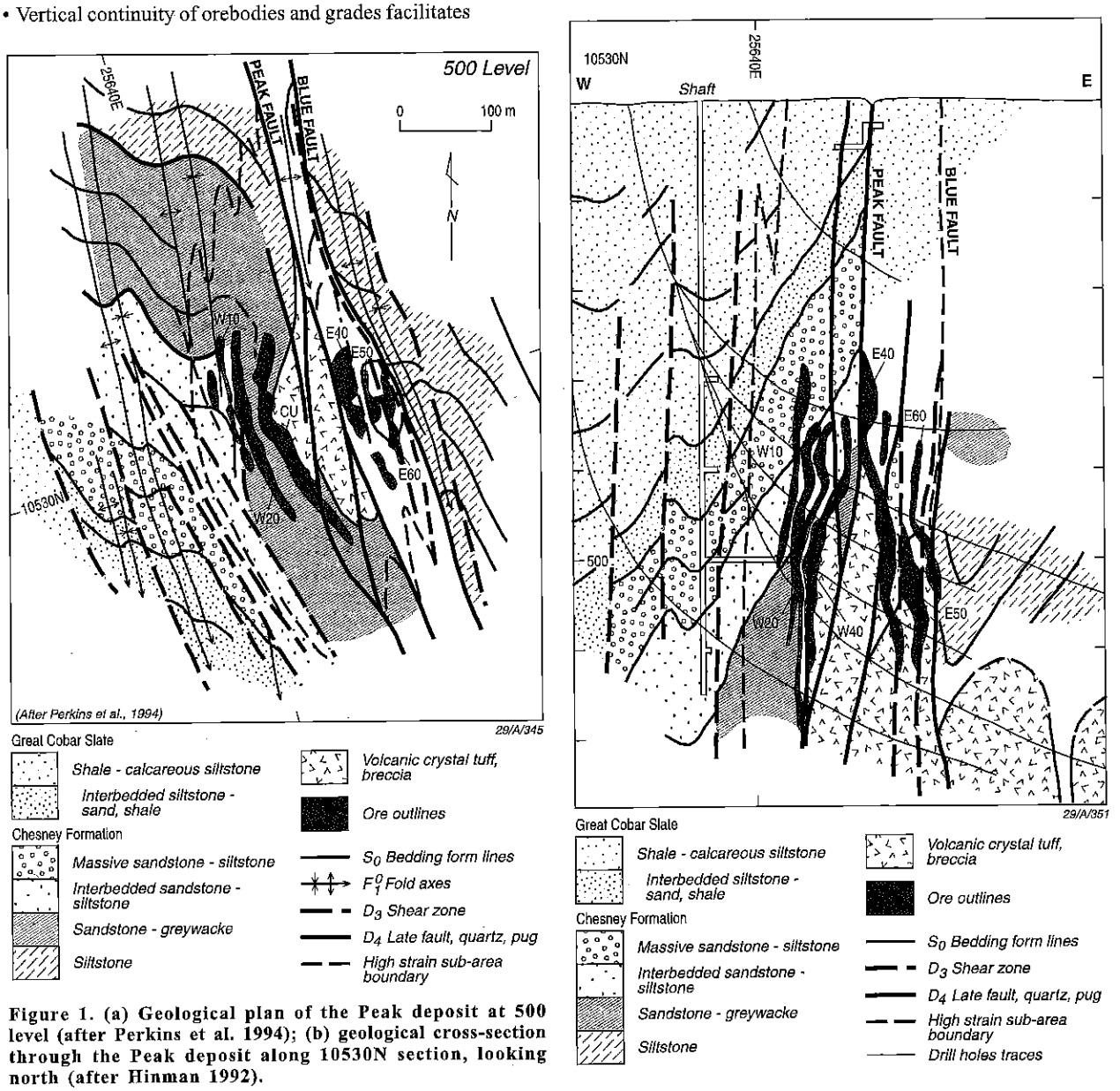

Figure 1. (a) Geological plan of the Peak deposit at 500 level (after Perkins et al. 1994); (b) geological cross-section through the Peak deposit along 10530N section, looking north (after Hinman 1992).

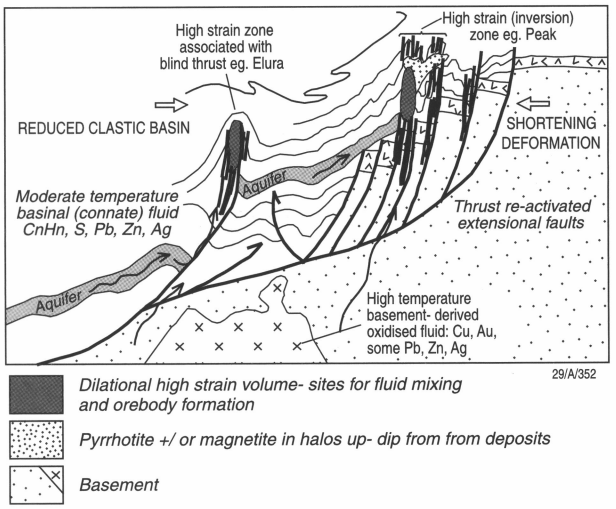

Figure 2. Schematic ore deposit model.

Geological criteria

- Deposits hosted in Late Silurian–Early Devonian Cobar Basin, an (inverted) extensional intra-continental ramp basin.
- Host sediments siliciclastic marine turbidites, minor felsic volcanics.
- Mineralisation occurred soon after sedimentation, synchronous with Early Devonian basin inversion.
- Inversion essentially reversed basin-opening stress regime: hence, reactivation of existing basin architecture.
- Deposits localised in steeply dipping, linear, ductile high-strain zones (minor reverse displacement), mostly adjacent to eastern basin margin; structures may link to shallow detachments at depth.
- At deposit scale, structural controls (dilational) include sites of marked competence contrast, doubly plunging (conical) anticlinal fold hinges, and fault jogs; on a regional scale, basement heterogeneities, and pre-existing extensional and transfer faults may be important.
- All orebodies elongate in the dominant stretching lineation (plunge subvertically–steeply north), and most aligned sub-parallel to or at low angle to (and are syn- to post-) the dominant regional cleavage.
- Lower greenschist facies metamorphism in high strain zones; upper diagenetic conditions in lower strain zones.
- At least one inversion zone reactivated as strike-slip and normal faults.
- Two episodes of mineralisation dated ($^{40}Ar/^{39}Ar$) at Peak deposit: syn-cleavage Cu–Au at 401.5±1.0 Ma, and replacive Ag–Pb–Zn at 384.0±1.4 Ma.
- No link to igneous rocks, with possible exception of McKinnons Au deposit.

Mineralisation features

- Epigenetic lodes, highly discordant to stratigraphy, occur as vertically continuous (>400 m), narrow (< 100 m, commonly <30 m) pipes, lenses and veins of short strike length (<300 m).
- Regional metal zoning from Au–Cu, Cu–minor Au, and Au–Cu–Pb–Zn deposits in the south, to Cu–Zn–Pb–Ag, then Ag–Pb–Zn–(Cu) deposits northward.
- Vertical and lateral metal zoning common within individual lodes.
- Complex weathering and oxidation (of sulphidic orebodies in particular) has resulted in near-surface depletion zones and supergene enrichment zones at depth.
- Gangue minerals include quartz, chlorite, carbonates, albite, sericite, barite.
- Orebodies mostly sulphidic, but couple are siliceous.
- Magnetite occurs in some Au–Cu orebodies; pyrrhotite occurs in parageneses with Ag–Pb–Zn mineralisation.

Alteration

- Lateral and vertical zonation in alteration envelopes: outer envelopes characterised by destruction of detrital chlorite and albite, and growth of ankerite ± siderite + quartz + chlorite ± pyrrhotite.
- Proximal (<50 m) silicification + chlorite, and quartz–carbonate veining, + albite + sericite, ± stilpnomelane, ± barite.
- Late-stage black chlorite occurs in late extensional (Peak) and reverse (CSA) shear/fault zones that are host to replacive Ag–Pb–Zn mineralisation.

Deposit geochemical criteria

- Visible alteration haloes up to 150 m above, and up to 1.5 km (typically <200 m) lateral to 'blind' deposits.
- Lateral depletion haloes of Li, Na, Rb, Sr and Ba at CSA, and Na depletion at Elura.
- Disseminated pyrrhotite anomaly up-dip, but offset from the Peak deposit.
- Cryptic stable isotope and major and trace element haloes developed above and lateral to deposits (e.g. CSA).
- Significant trace elements: Bi, As, Sb, Ni, Cd, Hg, Ba.
- S isotopes generally vary from +4 to +13‰, indicative of sulphur source in host Cobar Basin metasediments.
- Pb isotopes indicate mixing of two end-member components: 'basement' Au (e.g. stage 2 at Peak) and 'basinal' Ag–Pb–Zn (e.g. Elura); same model age as for basin formation and inversion.

Surficial geochemical criteria

- Cobar region has undergone complex regolith development, with differential erosion or incomplete development of primary laterite profiles and differential overprint of younger weathering profiles, resulting in significant modification of primary geochemistry.
- Multiphase weathering processes have resulted in wide dispersion halos (Bi, As, Sb), involving mechanical and hydromorphic dispersion.
- Lag sampling in erosional landforms has identified Pb–Zn–As (Cu) anomalies from known orebodies.
- Leached gossans with accompanying deeper level supergene enrichment in near-surface sulphidic orebodies (due to lowering of water tables and salinity increase).
- Some movement of metals through transported overburden by evapo-transpiration and root tapping.
- Ore discovered as siliceous gossans cropping out as erosional topographic highs.
- Weakly mineralised, strongly silicified zones retain primary metal assemblages in near surface.
- Possible biogeochemical anomalies (e.g. Cypress Pines—McKinnons deposit).

Geophysical criteria

- Host high-strain zones can be mapped in high-resolution aeromagnetic surveys (after processing to remove effects of extensive maghemite gravels).
- Some lodes have discrete bullseye magnetic anomalies, owing to presence and preferred orientation of pyrrhotite; e.g. Elura (Tonkin et al. 1988, Clark & Tonkin 1994).
- Both magnetite and pyrhotite in some deposits; e.g. Great Cobar, Chesney.

(Jeffrey & Thomson 1996).

Fluid chemistry and source

- n-alkane, and C_2H_4 hydrocarbons predominate in early stages at Elura, with CH_4-rich fluids (∞CH_4 = 0.3–1.0) dominant in later syn-cleavage stages at Elura and Peak.
- Low–moderate salinity (2–13 wt% NaCl equiv.), low–moderate temperature (T_h 100–220°C), H_2O–(n-alkane)–CH_4–CO_2, reduced (H_2S>SO_4) fluids interpreted as a basinal (connate) component; higher temperature (T_h 350–400°C), low–moderate salinity (0–7 wt% NaCl equiv.), high-temperature, pyrite-stable, more oxidised fluid interpreted as basement (metamorphic) fluid.
- At basinal scale, multiple fluid components recognised: basinal (connate) and basement (metamorphic) components dominant; possible meteoric and igneous components also identified.
- Relatively reduced (pyrrhotite +/or pyrite-stable) assemblages in Ag–Pb–Zn(–Cu) deposits; more oxidised (pyrite or magnetite-stable) assemblages in some stages of Cu–Au deposits.
- Precipitation mechanism: fluid mixing in extensional structural zones (rapid and repeated fluid depressurisation) at relatively shallow crustal levels.

et al., noting that the study by Jiang et al. (1995) does not satisfy the relative timing criteria established from field relationships. The significance of Jiang's dates is unknown.

- Jiang et al. (1995a,b) give isotopic data that suggest early fluids at Peak and Chesney were meteoric in origin and that later fluids were metamorphic. These data contrast with the paragenetic, fluid inclusion and Pb isotope data of Hinman (1992), which suggest early fluids were derived from the basin and later fluids were of mixed metamorphic–basinal origin.
- Marshall (1989) argued that mineralisation at CSA may be prestructural (late diagenetic) on the basis that much of the ore is deformed (although the ore parallels cleavage, and some ore cross-cuts cleavage (Brill 1989)).

Additional comments

Further isotope and dating studies are required to resolve questions over the origin of fluid components within the Cobar deposits. The complexity of these deposits necessitates that these studies be structurally and microstructurally constrained, and take into consideration multi-stage parageneses and spatial variations due to mixing.

Introduction

The Cobar district, in western New South Wales, is host to several small to medium, sediment-hosted polymetallic precious- and base-metal orebodies (Au–Cu–Ag–Pb–Zn). Gold and base metals have been mined there since 1870, and production (to end 1995) has been calculated at 2.5 million ounces Au, ~0.6 Mt Cu, 1500 t Ag, 0.6 Mt Pb, and 1.2 Mt Zn (Stegman & Stegman 1996). The metal content of the known deposits has been estimated at 1 Mt Cu, 1.6 Mt Pb, 2.6 Mt Zn, 4000 t Ag, and 70 t Au (Schmidt 1990). One new deposit (McKinnons) has been discovered in the 1990s, while deep drilling at existing deposits continues to add to ore reserves. Production in 1997 was from the Elura (Pb–Zn–Ag), CSA (Cu–Ag–Pb–Zn), Peak (Au–Cu), and McKinnons (Au) mines.

Cobar deposits differ substantially in orebody characteristics and geological setting from the other four main polymetallic sediment-hosted deposit types (MVT, stratiform shale-hosted deposits, Irish style Pb–Zn, and Broken Hill-type deposits). While individual deposits, and lodes within deposits, vary in aspects such as metal ratios, there is sufficient similarity in their epigenetic character, deposit shape and geometry, structural control, relative timing of formation (syn-basin inversion), complex multi-stage parageneses, hydrothermal fluid components and conditions of deposition for them to be grouped as a distinctive type of deposit (Glen 1987, 1995; Lawrie 1991a). The Au-rich Cobar deposits differ significantly from slate belt-hosted quartz vein deposits, such as the Victorian Au vein deposits, in that the latter are derived from CO_2-rich metamorphic fluids and form late in the orogenic cycle, often after peak metamorphism (Phillips & Powell 1993).

This review summarises the main features that define 'Cobar-style' deposits and reviews the key factors critical to the genesis of the known deposits. Exploration methods that might be used to find analogous deposits both within the basin and in other terranes are also reviewed.

Geological setting

Basin architecture

The Cobar Basin is one of a number of intra-continental basins in western New South Wales that opened in response to widespread back-arc extension of the Lachlan Fold Belt of eastern Australia. In the western portion of the Lachlan Fold Belt, this extension event was marked by emplacement of Late Silurian (S- and some I-type) granitoids, followed by basin initiation and sedimentation from the latest Silurian to the end of the Devonian (Glen et al. 1996).

The Cobar Basin is elongate, roughly N–S, about 150 km long and 50 km across (Fig. 3). Although it has been variably modified by crustal shortening, the basin fill is estimated to have been originally up to 6 kms thick (Glen et al. 1994). The basin is fault-bounded on all sides and structural analysis of basin/basement boundaries suggests that all the bounding faults are reactivated (inverted) syn-sedimentary growth faults (Glen 1990, Glen et al. 1994). On the east it has an oblique-slip faulted edge, with evidence of both imbricate thrusting and strike-slip movement on basin-bounding and within-basin structures (Glen et al. 1996).

Cobar Supergroup sediments in the basin unconformably

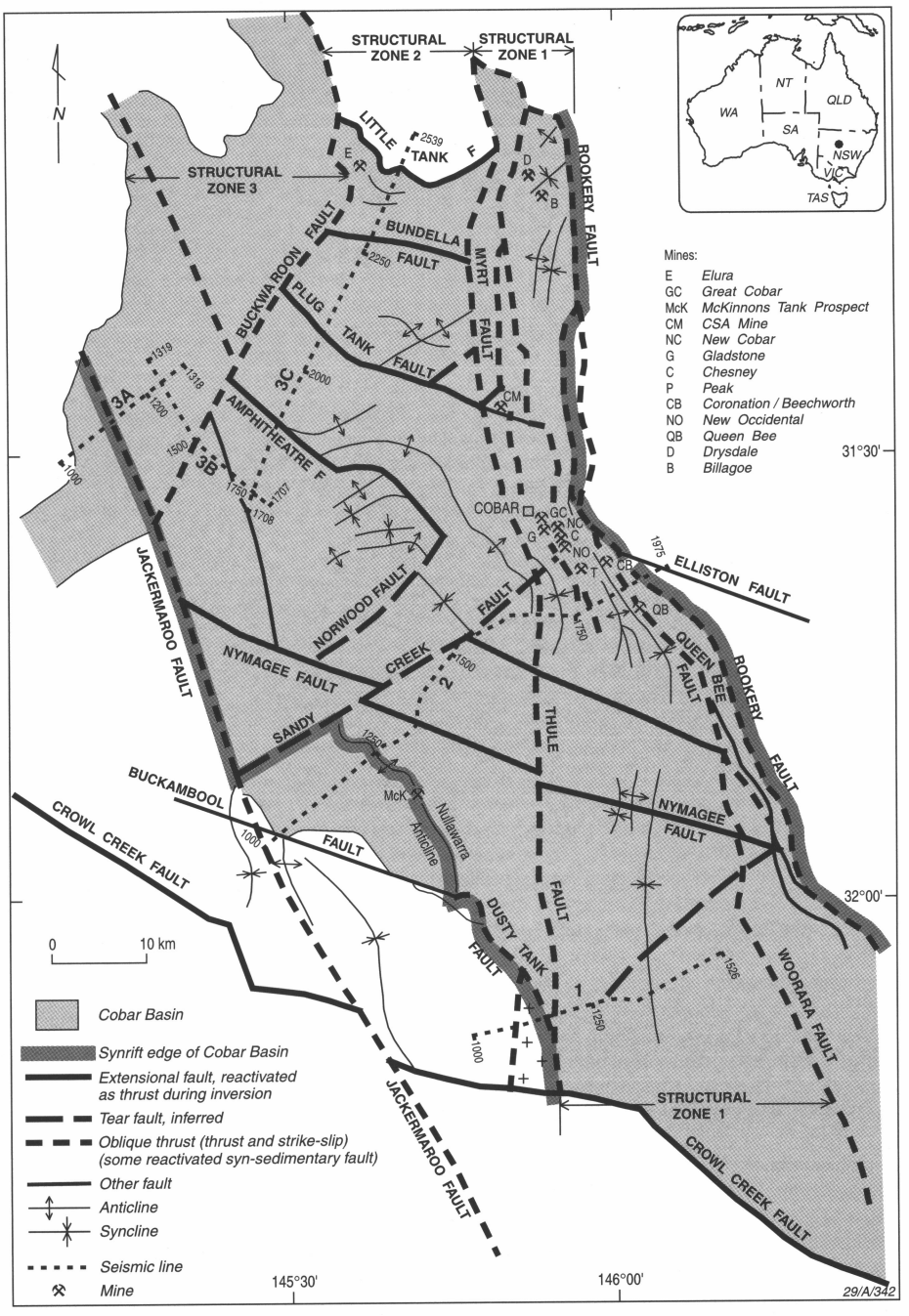

Figure 3. Extent of the Cobar Basin and major structural elements and deformation zones (after Glen (1990).

overlie ductily deformed greenschist–amphibolite facies metasediments and minor metavolcanics of the Cambro-Ordovician Girilambone Group and foliated S-type granitoids dated at 440 Ma (Pogson & Hillyard 1981). Nymagee Igneous Complex (Fig. 4). Cobar Supergroup metasediments also display unconformable relationships with a suite of post-kinematic Silurian (422–416Ma; Pogson & Hillyard 1981) granitoids that are mostly S-type, with one I-type noted. There are no known intrusions contemporaneous with mineralisation in the Cobar Basin, although the presence of advanced argillic alteration assemblages (Bywater et al. 1996) adjacent to the McKinnons Gold mine, towards the western margin of the basin, may indicate a possible link to intrusions at depth.

Host lithology

The Cobar Basin is filled predominantly with siliciclastic turbidites of the Cobar Supergroup. The basin has a crudely defined two-stage fill, with a lower part characterised by coarser grained clastics and more thickly bedded sediments than the upper portion (Glen et al. 1996). A two-stage, fining upwards sequence is not expected for extensional ramp basins, and may be a response to a higher heat flow regime on a larger crustal scale at a late stage in the basin history (Glen et al. 1996).

Most deposits near the town of Cobar occur in upwards-fining, easterly derived Nurri Group metasediments (e.g. Great Cobar Slate and Chesney Formation), which were deposited along the eastern margin of the basin. The overlying and more regionally extensive westerly derived turbidites of the Amphitheatre Group consist of a two-cycle sequence, with a lower upwards coarsening sequence and an upper thinly bedded sequence of finer grained lithologies (Glen et al. 1996). The lower part of the Amphitheatre Group (CSA Siltstone) is host to the CSA and Elura deposits (Glen 1987, Schmidt 1980, 1990, Hinman & Scott 1990).

Felsic volcanics are a minor part of the sequence; they occur in the Chesney Formation on the eastern side of the basin and as tuff bands in the CSA Siltstone Formation. Flow-banded rhyolites, interbedded crystal tuffs and rhyolitic volcanic breccias occur in the Peak deposit (Hinman & Scott 1990); however, there is some debate over whether these represent allochthonous thrust slices (Hinman 1994, Perkins et al. 1994) or intrusive bodies (Jiang & Seccombe 1995, Stegman 1998). Importantly, bedding in the rhyolites and crystal tuffs is discordant to bedding in the surrounding sediments (Hinman 1992). While tectonic breccias are developed at most contacts with sediments (Hinman 1992), Stegman (1998) has demonstrated that the rhyolites have intrusive contacts and geometry. The volcanics are locally altered and mineralised within the syn-mineralisation shear zone, and contain the regional S_1 cleavage (Hinman 1992, Stegman & Pocock 1996, Stegman 1998). This would appear to rule out a late tectonic intrusive origin for the rhyolites (Jiang & Seccombe 1995) and a pre-D_1 intrusive origin is favoured (Stegman 1998). There is no apparent temporal or spatial association between any other deposits and known igneous intrusions, although there is possibly indirect evidence at the McKinnons deposit (Bywater et al. 1996).

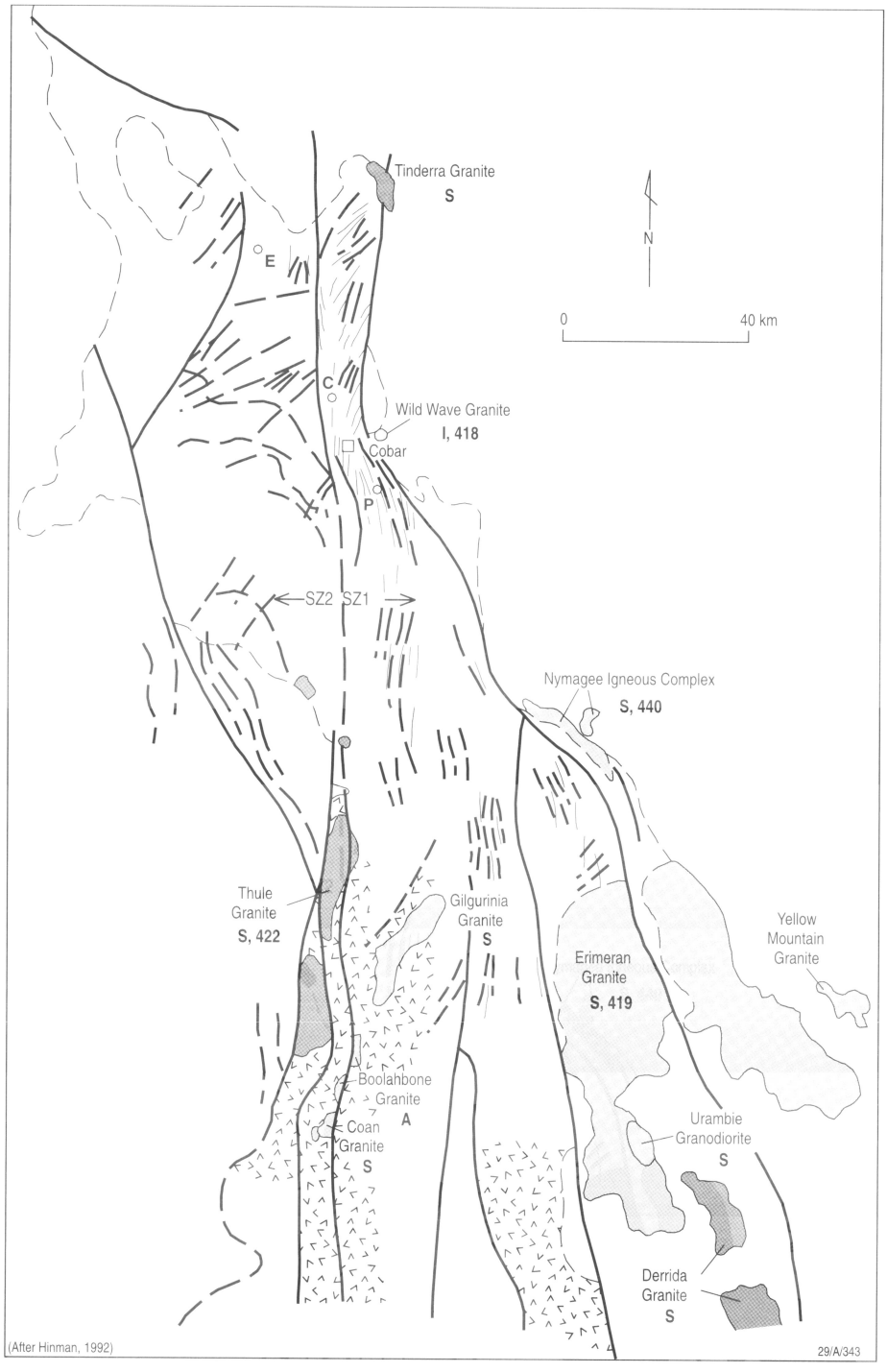

Figure 4. Distribution of major structures and granites in basement underlying the Cobar Basin (after Hinman 1992).

Structural history

Within the basin, three distinct structural domains, characterised by variation in deformation intensity and structural style and orientation, have been recognised (Fig. 3; Glen 1990, 1991). Most of the known base-metal and precious-metal deposits are hosted within siliciclastic metasediments, in a narrow corridor at the eastern margin of the Cobar Basin (structural domain 1, Glen 1990). The eastern and northern margins of the basin are characterised by penetrative cleavage development, although detailed mapping in these domains has identified discrete zones of high strain and more brittle faults (Andrews 1913, Sullivan 1947, Mulholland & Rayner 1961, Glen 1990, Hinman 1991a, 1992, Lawrie 1989a,b, 1990a, 1991, Gilligan & Byrnes 1995). The high-strain zones are up to several hundred metres wide (but can narrow to less than 5 m) and can be traced along strike for tens of kilometres. Brittle-fault structures are commonly located in these high-strain zones, with kinematic analysis supporting periodic reactivation and longevity of movement along some of these zones (Glen 1990, 1991, Hinman 1992, Stegman & Pocock 1996).

Seismic reflection profiles across the Cobar Basin have demonstrated that the ductile high-strain and brittle–ductile fault zones dip steeply east or west and appear to link to gently dipping structures at relatively shallow crustal depths (Drummond et al. 1992, Glen et al. 1994). Synthesis of surface structural data and seismic reflection data supports a thin-skinned tectonic, linked thrust fault interpretation for the major high-strain zones and faults (Glen et al. 1994, Glen 1995). Glen et al. (1996) argued that these data, when combined with gravity data (Spencer et al. 1992) and analogue modelling (Smith 1992), suggest oblique opening and closing of the Cobar Basin to the northeast and southwest. Seismic reflection profiles indicate that the Cobar Basin is not a classic rift basin, as there do not appear to be any faults at the base of the basin that link to the principal mid-crustal reflector. Rather, the basin most likely developed by flexure above a ramp in the mid-crustal detachment during crustal extension (Drummond et al. 1992, Glen et al. 1994).

Crustal shortening, which resulted in inversion of the Cobar Basin, occurred both along new thrust faults and by reversal of movement on existing syn-sedimentary extensional structures, which included primary growth (normal) and transfer (accommodation) faults (Glen 1990, 1991, Glen et al. 1996). Glen (1995) discriminated between thrust faults that are significant structural and stratigraphic breaks (thrust 'plates'), and zones of imbrication within plates.

Metamorphism of the basin

Metamorphism in the area is generally chlorite grade (Glen 1985, 1990). Based on illite crystallinity studies, Brill (1988a,b) established that metamorphic conditions in the vicinity of the majority of deposits are transitional between anchizone and epizone (transitional between diagenesis and low-grade metamorphism) and that further north, around the Elura deposit, conditions are anchizonal. Similarly, observed changes in b0 values, which suggest a gradation from low to intermediate pressure from north to south, are thought to be related to higher strain in structural domain 1 (Glen 1990).

Vitrinite reflectance data suggest that the basinal sediments were heated to conditions of burial diagenesis, but were exposed to hotter fluids in the high-strain zones associated with the ore deposits (Robertson & Taylor 1987). The timing of metamorphism is constrained by whole rock $^{40}Ar/^{39}Ar$ dating, which indicates metamorphism synchronous with a low-grade cleavage-forming event between 395 and 400 Ma (Glen et al. 1992a).

Mineralisation and alteration

Details of metal ratios, orebody shape, ore and alteration mineralogy and paragenesis, fluid characteristics and references for more detailed studies are presented in Table 1. All the deposits are paragenetically complex, and structural and microstructural analysis has been critical in resolving the timing of mineralisation and associated hydrothermal alteration relative to the spatial and temporal development of the shear zones, and relationships to host lithologies (O'Conner 1980, Glen 1987, de Roo 1989a, Lawrie 1989a,b, 1990a, 1991a, Hinman 1989, 1991a,b, 1992, Hinman & Scott 1990, Stegman & Pocock 1996). These studies provide the necessary constraints for understanding the geochemical evolution of the deposits and give a framework for isotopic dating studies (Perkins et al. 1994). Structural analysis is also a vital component of exploration models in the area (Lawrie 1989a, 1990a, Stegman & Pocock 1996).

Relationship of deposits to structure

Some of the earliest workers in the Cobar District mapped an association between mineralised lodes and gossans, and zones of penetrative cleavage development and associated faults (Andrews 1913, Sullivan 1947, Mulholland & Rayner 1961). There is now a general consensus that the Cobar deposits are epigenetic (most orebodies are highly discordant to host lithologies), that the bulk of the mineralisation formed synchronously with the formation of zones of penetrative cleavage development, and that the shortening deformation is related to inversion of the Cobar Basin (Glen 1987, 1991, 1995, de Roo 1989a, Hinman 1991a, Lawrie 1991, Perkins et al. 1994). An exception is a style of Ag-rich, Pb–Zn mineralisation that occurs as discrete lodes associated with a distinctive, desilicifying, black chlorite–muscovite replacement at the Peak deposit. Kinematic evidence and minor normal displacement demonstrates that this style of replacement mineralisation is associated with relaxation, normal fault reactivation of structures within the shortening zones (Hinman 1992, Perkins et al. 1994).

The high-strain zones that host the major deposits are characterised by development of a variably penetrative cleavage, which ranges from a slaty cleavage to a solution cleavage. These structures are relatively linear in character, but vary in width from a few hundred metres to less than 10 m. However, not all subparallel high-strain zones are mineralised, and those that are tend to be mineralised only in specific segments/volumes of extreme high strain. Near Cobar the major deposits occur along two principal structures, the Great Chesney Fault and the Great Peak Fault (Fig. 3). These are significant structural and stratigraphic thrust 'plate' discontinuities (Glen 1995). Mineralisation along these structures occurs primarily where strain heterogeneities are localised either by intersection with pre-existing structures or around lithological heterogeneities or favourable bedding geometry (Glen 1987, 1995, Lawrie 1991, Hinman 1992).

Elsewhere, deposits occur in zones of imbrication within thrust plates. Examples of within-thrust plate deposits include the Great Cobar, Dapville and Mount Drysdale deposits in the central area (Glen 1995). In the northern part of the basin, examples include the CSA deposits, which occur in a zone of several subparallel imbricate structures, and the Elura deposit. Drilling above the deeper northern orebodies at Elura has revealed that deformation intensity, alteration and mineralisation die out rapidly upwards away from the orebodies, suggesting that the mineralisation is developed at the tip of a blind thrust (Lawrie 1989a, Glen 1991).

Discrete orebodies are localised along the strike of individual thrusts/ high-strain zones within a range of dilational geometries, where there are anisotropies developed in the stress systems during basin inversion. Structural traps include fault jogs, horsetail splays at fault terminations, and areas where there are marked differences in competency (lithology) contrasts across fault boundaries (Mulholland & Rayner 1961, Glen 1987, 1995). These contrasts led to deformation partitioning and doubly plunging folds developed in high-strain volumes (Hinman 1991a, 1992).

At the eastern margin of the basin, the most economically significant structures trend just west of north, while those in the northern half of the basin trend more NW–WNW (Glen 1990,

Stegman & Pocock 1996). At Elura, the mineralised high-strain zone overall now has a NNW strike, an orientation that is partly a function of dextral offsetting by a number of later subparallel NNE–NE-striking transpressional shear zones (Lawrie 1989a). In both the Peak and Elura deposits, vein orientations record episodic shifts in the principal stress axes within the main deformation event, synchronous with mineralisation, with a progressive rotation in the stress system also recorded. At Elura, the principal stress axis was initially oriented to produce a cleavage with a WNW strike, with a shift to a more NW strike during the main cleavage-producing deformation event (Lawrie 1989a).

Not all structures with the same relative age and orientation are mineralised, and orebodies in the same structure may have different ore and alteration parageneses (Table 1). Where these shear zones have been studied in detail, as at Elura and at Peak, a reverse sense of movement synchronous with most mineralisation is indicated by a subvertical stretching lineation and lithology displacements (de Roo 1989a, Lawrie 1989a, Hinman 1992).

All the known orebodies are elongate in the dominant stretching lineation, which plunges steeply to the north in the high-strain zones (Fig. 5; Russell & Lewis 1965, Lawrie 1989a, Hinman 1992). Most deposits have considerable vertical extent (>400 m, often >1k m) and occur as narrow (< 100 m, commonly <30 m) pipes, lenses and veins, of short strike length (<300 m; see Glen 1995 for maps and cross-sections; Figs 1, 6,).

Orebodies at Elura and Peak are localised where vertical extension in the high-strain zones is extreme, and individual lodes form within doubly plunging anticlines that have sheath-like geometry (Figs 1, 6, de Roo 1989a, Lawrie 1991, Hinman 1992). These sheath folds form under anomalously high strain, with marked partitioning between high strain in fold limbs and relatively low strain within fold hinges. The along-strike heterogeneity in vertical extension is illustrated in long sections through the Elura and Peak orebodies (Figs 5, 6d; Lawrie 1990b,c, Hinman 1992). Low-grade vein-style mineralisation occurs between many of the individual orebodies in all the main deposits.

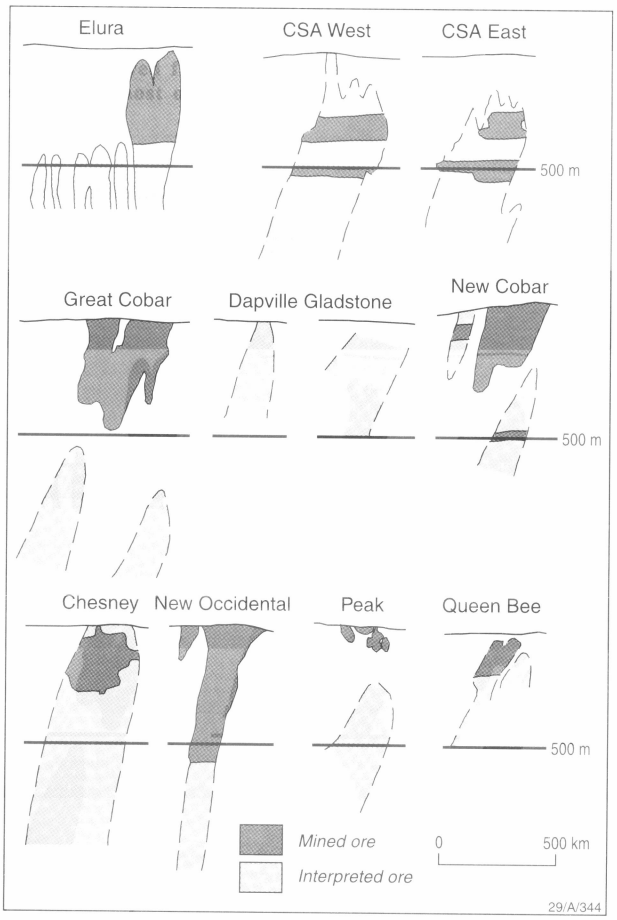

Figure 5. Longitudinal sections through the main Cobar deposits viewed from the west. A steep northerly plunge is evident in most ore bodies.

The geometry of host structures for these orebodies is not simple. At upper levels in the Elura mine, both massive replacement and vein-style mineralisation are hosted within culminations in an anticlinal hinge zone (Fig. 6). At depth beneath the two main orebodies, mineralisation becomes more vein-style and semi-massive, with cleavage much less intensely developed in the fold culminations. The main fold structure is vertically continuous for at least 900 m (de Roo 1989a, Lawrie 1989b); however, below 5 level in the mine (500 m below ground surface), the principal anticlinal fold structure has degenerated into a more complex structure, with up to three principal parasitic anticlines present at 5 haulage level (Fig. 6b; Lawrie 1989a). Massive sulphide mineralisation is localised in the hinge zones of these parasitic structures at depth, with the orebodies occurring as discrete and subparallel bodies (Fig. 6b,d). This strong structural control on mineralisation is reflected in the outline of economic orebodies and metal zonation within the deeper parts of the orebody (Lawrie 1990b, 1991b).

An earlier suggestion that the two main southern Elura orebodies formed in culminations formed by the intersection, approximately at right angles, of two sets of upright folds (de Roo 1989a) is not supported by microstructural or macrostructural evidence (Lawrie 1989a,b). At Elura, close fold hinges, which parallel (and developed synchronously with) the mineralised structure, do not develop curviplanar hinges, show no evidence of an earlier set of cross-structures, and are characterised by a weakly penetrative cleavage in their limb zones.

In contrast, the markedly curviplanar fold hinges within which the individual lodes occur are bounded by high-strain zones of intensely penetrative cleavage and strongly sheared bedding in fold limbs. That these doubly plunging structures are a product of fold development within one shearing event is further demonstrated above the northern Elura orebodies, where deformation intensity dies out upwards, so that there is little evidence for the presence of any penetrative cleavage and no doubly plunging fold culminations 150 m above the tops of the orebodies (Lawrie 1990; Fig. 6c). The syn-mineralisation (S_2) cleavage on the limbs of the anticline is a penetrative slaty cleavage. However, this changes in character upwards and is a spaced solution and/or weakly developed slaty cleavage 200 m above the orebodies. Up dip, bedding is relatively undeformed, and only locally cross-cut by a weak solution, slaty or fracture cleavage. At the surface, 450 m above the orebodies, the anticline persists with a NW-striking hinge zone; however, the hinge line is only weakly curviplanar (Lawrie 1989a, 1990a). Although the anticline can be traced, it was not possible to discern a high-strain zone above that developed at depth.

NNE- to NE-trending brittle–ductile shear zones offset and post-date mineralisation and alteration at CSA (Scott & Phillips 1990) and Elura (Fig. 6b; Lawrie 1988, 1989a,b). At Elura, these later shear zones tend to partition around the orebodies, owing to the siliceous nature of the proximal alteration envelopes, and are focussed as narrow (<20 m wide) zones into the less-altered portions of the pre-existing mineralised high-strain zones. This partitioning of strain leads to minimal remobilisation of ore in the massive sulphide orebodies during the later shearing event.

Although there is no apparent difference in chemical composition between host metasediments in the basin, there are important differences in bed thickness and the scale of interbedding of sandstone/siltstone/shale horizons, and this also contributes to final orebody geometry. Vein-style deposits are noticeably developed in relatively homogeneous lithologies with little interbedding. More lensoidal orebodies are developed where there is greater lithology contrast, and pipe-like orebodies are developed in rythmically interbedded turbidites (Lawrie 1989a). This is almost certainly a function of shearing across bedding to

Table 1a. Orebody characteristics from mines producing in 1997

Deposit	*Peak*	*Elura*	*CSA*	*McKinnons*
Main metals	Au–Cu–Pb–Zn–Ag	Ag–Pb–Zn–(Cu)	Cu–Zn–Pb–Ag	Au (minor Ag)
Tonnage	Resources @ July 1995: 4.6 Mt @ 8.8 g/t Au, 0.8% Cu, 1.1% Pb, 1.0% Zn, 8.4 g/t Ag	Production to 1995: 1190 t Ag, 0.54 Mt Pb, 0.89 Mt Zn, 0.012 Mt Cu, 88 000 oz. Au Reserves @ 1996: 33 Mt @ 5.6% Pb, 8.6% Zn, 135 g/t Ag	Production to Dec 1995: 20 Mt @ 2.11% Cu, 0.62% Pb, 1.98% Zn, 22 g/t Ag Resources @ Dec 1995: 15 Mt @ 3.97% Cu, 0.15% Pb, 0.55% Zn	Reserves @ Dec 1994: 2.5 Mt @ 1.73 g/t Au
Orebody geometry and dimensions	Several discrete lenses and pods 3–25 m wide, 50–250 m long, 300–700 m deep. Subvertical (N) plunge to lenses.	At least 7 ellipsoidal pipes; 40–100 m across, vertical extent of largest pipe >600 m. Plunge >85° N.	Subparallel, discontinuous veins and lenses (locally termed 'systems'); vertically continuous to >2 km.	Isolated high-grade lodes within lower grade envelope.
Metal zonation	Crude outward zonation from Cu to Pb–Zn. No documented vertical zonation, but internal zoning within lodes.	Marked lateral and vertical metal zonation with similar metal ratios at equivalent elevations in each pipe; increase in Cu and decrease in As, Ag with increasing depth.	Each vein 'system' characterised by distinctive metal ratios. Marked vertical zonation: increase in Cu and decrease in Pb, Zn with depth; lateral zonation with Pb, Zn peripheral to Cu at depth.	Au near surface only (<60 m), zoned to Au+Ag, then Pb, Zn, Ag at depth and northward.
Ore mineralogy and alteration paragenesis	Five-stage paragenesis* (Hinman 1992): (1) disseminated pyrrhotite; (2) quartz–calcite–pyrite veins; (3) silica + Ag-poor, sphalerite–galena; (4) silica + Au-rich, pyrrhotite–chalcopyrite–(sphalerite–galena)–native Au–electrum–chlorite–muscovite; (5) silica-absent, chlorite–(muscovite), Ag-rich, sphalerite–galena–pyrrhotite–pyrite–(chalcopyrite). *Jiang & Seccombe (1994) proposed a 3-stage paragenesis (7 ore sub-stages).	Six-stage paragenesis: (1) carbonate + silicification + chlorite; (2) crack-seal + breccia quartz veins + carbonate; (3) framboidal pyrite + quartz; (4) quartz + pyrite + arsenopyrite + sphalerite; (5) sphalerite + galena + pyrrhotite ± pyrite–sericite–chlorite–dolomite; (6) Ag-rich tetrahedrite + tennantite + enargite + chalcopyrite + galena + pyrite + Ba-feldspar + chlorite + albite. *Cryptic alteration halo extends up to at least 500 m laterally and 300 m above pipes.	Multi-stage paragenesis, but no detailed description published: (1) Early depletion in alkalis and alkali earths (Robertson & Taylor 1987); (2) Chlorite + silica dominant alteration Early—silica + Fe-rich chlorite–chalcopyrite ± pyrite–sphalerite–pyrrhotite–galena; Later—quartz-poor, black Mg-chlorite + chalcopyrite. Most ore minerals parallel cleavage AND are deformed.	Multi-stage paragenesis: (1) Quartz–pyrite(+Au?)–silicification; (2) Pyrite–sphalerite–galena; (3) High-grade Au + chalcedonic silica in quartz breccias. Locally, digenite and covellite occur in argillaceous alteration assemblage.
Fluid-inclusion data	(3) T_h 150–360°C, low salinity (2–5 wt% NaCl equiv.), XCH_4 = 1–0.5 (CH_4–CO_2), L + V = heterogeneous entrapment, i.e. mixing; (4) T_h 300–350°C, max. salinity 4–6 wt% NaCl equiv., XCH_4 = 1.0, L + V = mixing; Max P(formation) = 800–1200 bars.	(2) H_2O + n-alkanes (T_h 120–160°C); (3) Liquid-rich H_2O + CH_4 + C_2H_6 + CO_2 (T_h <220°C) and liquid-rich, H_2O + Ca; (5) Liquid-rich, mod. salinity (max. 13 wt%), H_2O–CH_4–CO_2 T_h 220–270°C; (6) low salinity (max 6%), more vapour-rich, H_2O–CH_4–CO_2 (T_h 330–380°C).	No published data	No published data
Isotope data	O (silicified sediments): 11.1–12.6. O: –4.6 to 1.6 (Pb–Zn–Ag stage); D: –110 to –68 (Cu–Au stage); Pb: mixing of basinal + basement signatures.	S: 4.7–12.6 (host sediments) $^{206}Pb/^{204}Pb$ = 18.13	$^{206}Pb/^{204}Pb$ = 18.11	No published data
Structural control	Basement heterogeneity localises high-strain volume; intersection of NW-trending high-strain zones with basin aquifer. Doubly plunging anticlines. Stage 5 normal faults.	Hosted in NW-trending D2 high-strain zone at tip of blind thrust; orebodies localised in cores of doubly plunging anticlines, developed where extension is localised at the intersection with NE-trending basement heterogeneities.	Veins and podiform lenses distributed as subparallel or en-echelon lodes hosted in shear zones	Hosted in NW-trending zone; high-grade lodes occur at intersection of NW and NE-trending (brittle–ductile) structures.
Structural timing	Stages 1–4 syn to late D2 shortening; Stage 5 syn-brittle extensional faults.	All stages syn to late D2 shortening deformation.	Early syn-regional cleavage.	Synchronous with deformation.
References	Hinman & Scott 1990, Hinman 1992, Perkins et al. 1994, Jiang & Seccombe 1994, 1995, Jiang et al. 1995a,b.	Schmidt 1980, 1990, de Roo 1989a, Lawrie 1988, 1989a,b, 1990a,b,c, 1991.	Scott & Phillips 1990, Brill 1988a, Marshall 1989, McDermott et al. 1996, Binns & Appleyard 1986.	Bywater et al. 1996.

Table 1b. Orebody characteristics from historical workings.

Deposit	*Chesney*	*New Cobar*	*New Occidental*	*Great Cobar*
Main metals	Au–Cu	Au–Cu	Au	Cu–Au
Deposit size	Production: 28,490 oz Au, >1110 kg Ag, 6214 t Cu	Production 242,510 oz Au, >860 kg Ag, >5052 t Cu (0.8–1.2% Cu)	Production: 691,420 oz Au. (0.1–0.2% Cu)	Production 293,470 oz Au, 46,700 kg Ag, 114,826 t Cu
Orebody shape/dimensions	Four lodes: two pipe-like bodies (Au) 30 x 20 m, connected by vein-style lode (Cu) 150 x 10 m. These are continuous to 250–300 m. Fourth lode 200 x 3 m. All pipes plunge steeply N.	Four pipe-like orebodies: 3–6 m x 50–200 m deep; 6–12 m x 60–80 m to 400 m deep; 6–12 m x 80–>700 m deep; 2–5 m x 50 m, 200–>500 m deep. All pipes plunge steeply N.	Six discrete lenses within a disc-shaped orebody 200 x 25 m, continuous to >1200 m deep. All lenses plunge steeply N.	Three pipe-shaped lodes: 110 x 30 m; 130 x 25 m and 45 x 15 m. Vertical continuity >1000 m. All pipes plunge steeply N. Four smaller lenses to E.
Metal zoning	Metal ratios vary between individual lodes.	Pyrite halo; Au grades increase as lode dip shallows upwards; little variation in metal ratios between lodes.	Discrete lenses have different metal ratios. High-grade Au–Bi–magnetite in upper portions of deposit.	Lateral zoning and vertical zoning—decrease in 'basic' ore and increasingly 'siliceous' with depth.
Ore mineralogy and alteration paragenesis	Six-stage paragenesis: Stages 1–5 quartz veins + silicification only; Stage 6: chlorite–chalcopyrite–pyrrhotite–magnetite–native Au–Ag–native Bi–bismuthinite; minor sphalerite–galena–pyrite.	Multi-stage paragenesis: (1) silicification; (2) pre-cleavage quartz veins; (3) chlorite–quartz veins and breccias; (3A) colloform quartz–magnetite–Au–Bi–bismuthinite; (3B) chalcopyrite–pyrrhotite–pyrite; (3C) galena–sphalerite–pyrrhotite.	Low-sulphide orebody, multi-stage paragenesis: (1) silicification; (2) quartz veining; (3) syn-cleavage quartz veins and breccias, colloform banded quartz–chlorite; (3A) chlorite + magnetite; native Bi–bismuthinite–Au–magnetite; (3B) chalcopyrite–pyrrhotite–quartz–pyrite; (3C) galena–Au–sphalerite–pyrite–pyrrhotite; (4) quartz–carbonate veins; (5) black chlorite + pyrite.	Three ore types recognised: (A) silicified and chloritised slate hosting magnetite–pyrrhotite–chalcopyrite (basic ore); (B) quartz–chalcopyrite–pyrrhotite–minor magnetite (siliceouus ore); (C) black chlorite + Pb–Zn mineralisation.
Fluid inclusion data	(1) 2.5–6.3% NaCl equiv., T_h 179–317°C; (2) 5.2–6.9% NaCl equiv., T_h 151–243°C; (3) 4.6–9.1% NaCl equiv., T_h 285–381°C; (4) 6.7–7.6% NaCl equiv., (5) T_h 298–408°C.	$^{206}Pb/^{204}Pb$ = 18.1	No published data	No published data.
Isotope data	(1) O:3.8 to 5.6 (chlorite); D –69 to –91.5; (2,3) O: 5.1 to 6.5 (chlorite); D: –66.6 to –92.8 (chlorite); (5) O: 8.0; C: 13.2 to 18.9 (calcite).	No published data	No published data	No published data.
Structural control	Shear-zone-hosted, S of warp in thrust contact and lithology contrast.	Shear-hosted; syn-shortening or left lateral jog (strike-slip reactivation of thrust fault).	Epigenetic. Shear-hosted at lithology/rheology contact; left-stepping jog.	Epigenetic.
Structural timing	Syn-cleavage	Syn-main cleavage	Syn-main cleavage (waning stage)	Syn-shear zone
References	Jiang et al. 1995a,b, Gilligan & Byrnes 1995, Stegman & Pocock 1996.	Mullholland & Rayner 1961, Glen 1987, Hinman 1992, Stegman & Pocock 1996.	Andrews 1913, Sullivan 1947, Mullholland & Rayner 1961, Glen 1987, Stegman & Pocock 1996.	Andrews 1913, Thomson 1953, Thompson 1969.

produce dilational geometry. In poorly bedded lithologies, internal shear geometry in ductile shear zones is the dominant structural control on mineralisation, whereas shearing at a high angle to bedding across rheologically disimilar interbeds permits gaping and leads on a larger scale to larger strain heterogeneities and the development of anticlinal folds, which may localise lensoidal and pipe-shaped orebodies.

Metal zonation

Within the Cobar Basin, known economic mineralisation and associated alteration are largely restricted to a 50 km long segment near the basin's eastern margin (Fig. 3). Metal zoning is recognised on a regional scale within this 50 km zone: there are Au–Cu, Cu–minor Au, and Au–Cu–Pb–Zn deposits in the south, shifting progressively northwards to Cu–Zn–Pb–Ag, then Ag–Pb–Zn–(Cu) deposits (Mulholland & Rayner 1961). There is an overall trend to less Cu–Au northwards (Glen 1987).

The McKinnons deposit (Bywater et al. 1996), which lies towards the western margin of the basin, is essentially a Au-only deposit with very minor Cu. It differs in several substantial orebody characteristics compared with the deposits in the east.

Differences in metal ratios are also observed along individual high-strain zones. An example is the Chesney Fault Zone, which is continuous for up to 35 km strike length (Stegman & Pocock 1996) and is host to several minor historical workings and a few larger deposits. Deposits include those that are Au-only (e.g. New Cobar), Au–Cu (e.g. Chesney), Cu–minor Au (Mt Pleasant, Young Australia, Wood Duck, Fort Bourke, East Cobar, Tharsis), Cu-only (Burrabungie), and Au–Cu–Pb–Zn (e.g. New Occidental). Gold and Cu–Au deposits hosted within the Great Chesney Fault and adjacent structures that host the Great Cobar and Dapville deposits are distinctive within the Cobar field, in that the ore is commonly associated with magnetite ± native bismuth and bismuthinite.

There are also marked differences in metal ratios between adjacent lodes within deposits. Moreover, both lateral and vertical metal zoning in individual ore lenses are observed (Lawrie 1990b, 1991a,b). At the Elura deposit, there is a relatively complex three-dimensional metal zonation superimposed on three concentric ore types (Fig. 7; Lawrie 1990b, 1991b). Vertical metal zonation is particularly well demonstrated at Elura, where an increase in Zn, Pb and Cu contents and a decrease in Ag and As contents are recorded with depth (Fig. 7). There are pronounced Ag caps and rims to the two main orebodies, with the cap zones of the two main deposits affected by supergene processes (Taylor et al. 1984).

Metal zoning in plan view is more complex (Fig. 7). The inner massive pyrrhotite-rich core is rich in Cu, Pb (as galena) and Zn, and depleted in Ag and As. In the upper levels of the orebodies the pyritic inner rims are particularly rich in As (arsenopyrite). The outer siliceous pyrite rim to the orebodies is notable for its very high Ag (as freibergite) and elevated Pb and Cu. The roughly concentric distribution of ore types (Schmidt 1990) and metal distribution (Lawrie 1990b) have been interpreted as a function of a combination of bedding control on replacement and, in particular, the early and preferential replacement of thicker sandstone beds, which have a similar distribution in the core of the sheath-like anticlines (Lawrie 1990b).

Hydrothermal alteration halos

Studies of major and trace elements and detrital minerals in host rocks near the Cobar deposits have identified both extensive depletion haloes, linked to destruction of detrital minerals and leaching of base metals, and narrower enrichment zones within the depletion zones, which are associated with new alteration mineral growth and polymetallic mineralisation (Robertson & Taylor 1987, Schmidt 1990). Depletion in alkalis and alkaline earths (e.g. Li and, to a lesser extent, Na, K, Rb, Sr, Ba) coincides with haloes of base-metal depletion in host rocks at the CSA, Chesney, Peak, Queen Bee and Tharsis deposits (Robertson & Taylor 1987). Alkali depletion has been linked to destruction of detrital feldspar and sericite, while depletion in Na and Li at Elura is associated with the destruction of detrital feldspar, sericite, chlorite and biotite (Schmidt 1980).

Vitrinite reflectance data show that, in the high-strain zones, detrital carbonaceous material is also depleted and is in the form of graphite (Robertson & Taylor 1987). However, host rocks near orebodies outside the high-strain zones contain minor amounts of detrital carbonaceous material, which is bituminous with a sub-anthracitic coal rank (Robertson 1974, Schmidt 1980, Saxby 1981). Carbonaceous material is locally concentrated in poorly developed 'proto- or dewatering cleavage' rather than in later penetrative slaty cleavage (Robertson & Taylor 1987).

The hydrothermal alteration (enrichment) haloes associated with the Cobar deposits are variably developed; however, even the Au-rich end-member deposits have substantial alteration zones relative to other deposit styles, such as slate-belt Au deposits. There is an overall similarity in the nature of wallrock alteration assemblages in the Cobar deposits (Table 1). Silicification is common in most deposits, and manifested as topographic ridges in the southern half of the field. Shale discolouration, the product of oxidation of pyrite, is also a common surface expression of alteration.

Narrower zones of intense silicification, with chlorite and sericite, are commonly found within 20 m of orebody contacts (Binns & Appleyard 1986, Schmidt 1980). Broader zones of

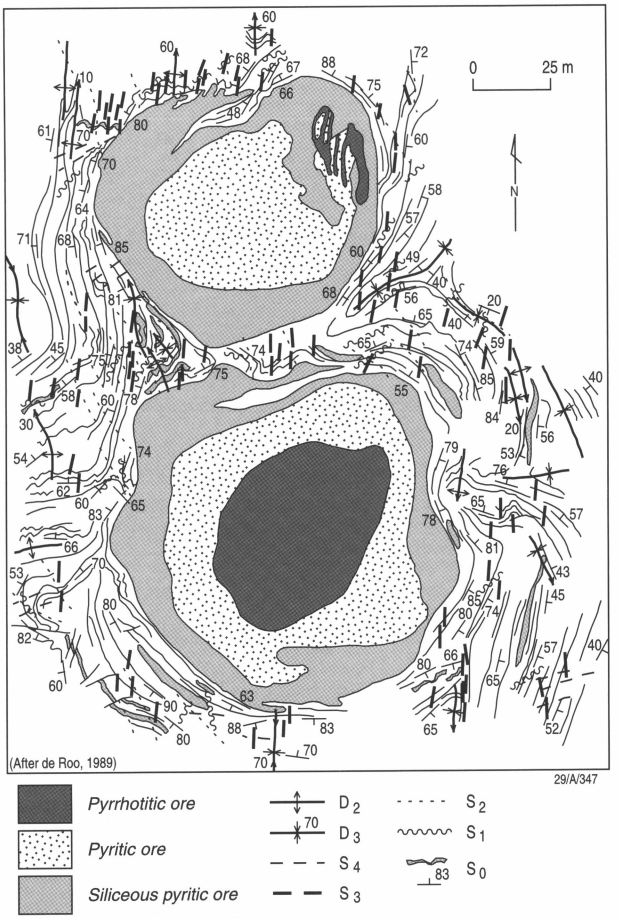

Figure 6. (a) Geological map of the two southerly Elura ore bodies at 3 drill level (after de Roo 1989a). (b: facing page) The Elura orebodies at 4 haulage level. The massive sulphide pods are enveloped by a semi-continuous envelope of silicification, semi-massive sulphide and vein ore. An envelope of carbonate spots (siderite and/or ankerite porphyroblasts) defines a visible outer alteration halo. Insets show a schematic cross-section (looking north) and a longitudinal section through the same ore bodies. After Lawrie (1988, 1989a).

cryptic alteration have been identified by whole rock and isotope geochemistry (Robertson & Taylor 1987, Schmidt 1990). Carbonate alteration (siderite and ankerite) defines a marked outer halo that is co-extensive with the main shear zone at Elura (Schmidt 1990; Fig. 6b). In contrast, there is no appreciable carbonate alteration except within or immediately next to the base-metal veins that form a minor component in the Cu–Au deposits.

Marked decreases in visible alteration are documented above the deeper CSA and northern Elura orebodies (Robertson & Taylor 1987, Lawrie 1990). At Elura the decrease in alteration correlates with a reduction in cleavage intensity, which dies out upwards (Lawrie 1989a, 1990a). Veining and pervasive silicification die out abruptly, less than 100 m above massive sulphide pods, and carbonate spotting and hydrothermal chlorite are present only in narrow solution and fracture cleavages 20 m above the northern orebodies.

Chloritic shear zones that post-date the main mineralising event are visible in many deposits. At Peak, a post main-stage

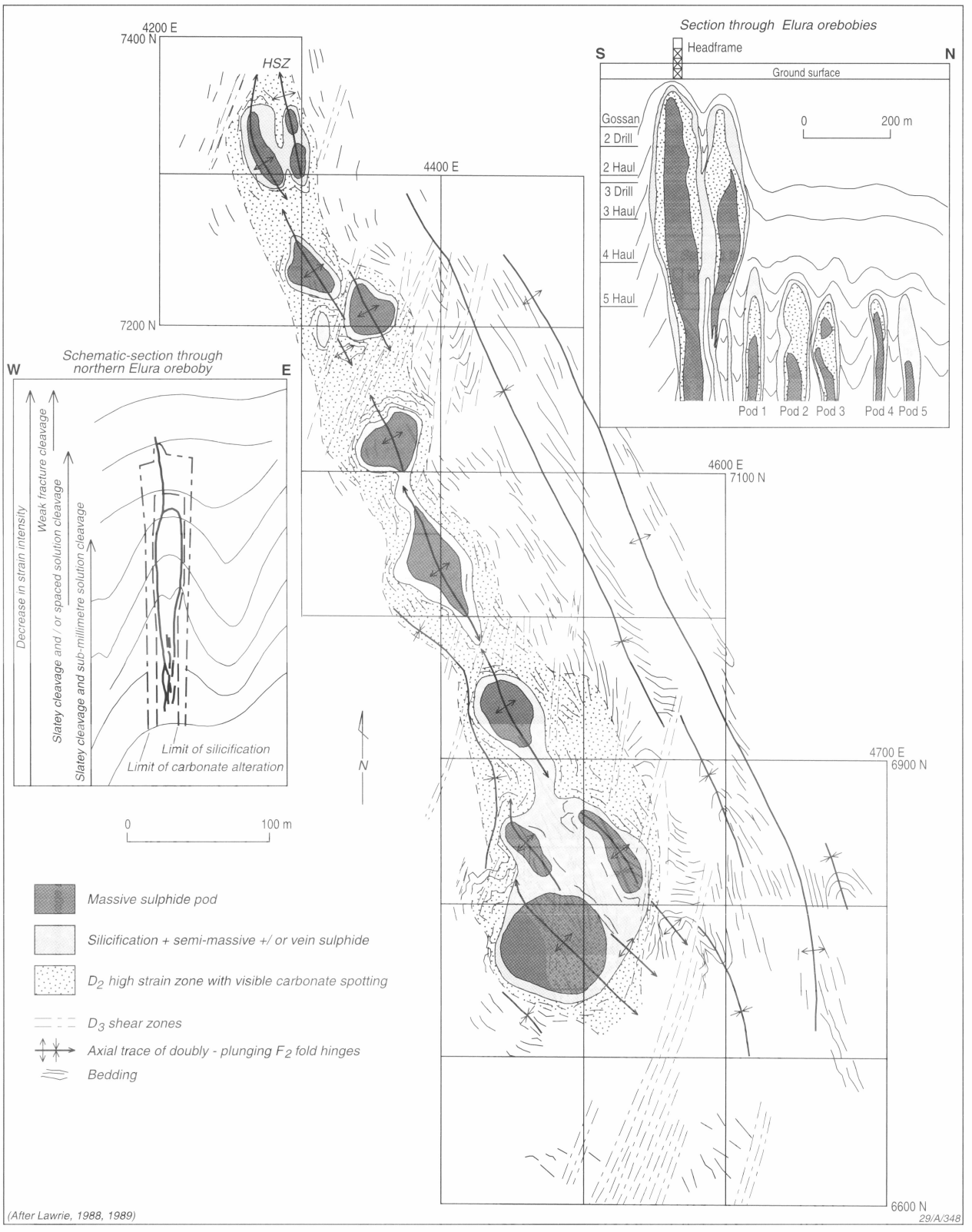

mineralising event, which comprises chlorite–muscovite replacement and Ag–Pb–Zn mineralisation, formed during extensional relaxation of earlier contractional structures (384 ± 1.4 Ma at Peak; Perkins et al. 1994) that post-date late-stage contractional chloritic shear zones. At Elura, orebody-related alteration assemblages have been destroyed in NNE-trending post-mineralisation chloritic shear zones (Fig. 6b). The latter are transpressional and dextrally offset the pre-existing mineralised structure. Focussing of these late shear zones between orebodies was due to partitioning of strain into less silicified areas, with the result that there was little remobilisation of ore during this late event.

Genetic model

Each known Cobar deposit is structurally controlled (Glen 1987, Lawrie 1991, Hinman 1991), and all appear to have formed at the same time relative to the inversion of the Cobar Basin (Glen 1987, 1990, 1991, Glen et al. 1992b, Lawrie 1991a, Hinman 1992, Perkins et al. 1994). Although individual deposits differ in the specifics of structural controls, the main deposits appear to share common structural elements in their genesis. Furthermore, comparison of fluid data from the Elura and Peak deposits, which have the most extensively documented paragenetic and deformation histories, and which lie towards the opposite ends of the spectrum in terms of metal ratios, orebody shapes and host rocks, suggests that a common genetic model links the Cobar polymetallic orebodies. The components of this model are discussed below.

Host rocks

The Cobar deposits occur in reduced (although not notably carbonaceous) siliciclastic turbidite sedimentary units, none of which is particularly unusual in chemical composition relative to other sequences in the basin. This suggests that Cobar-style deposits may occur anywhere in the basin provided the component fluids are channelled along the requisite (high strain) permeability zones. Orebodies form at sites where the key fluid components are focussed into favourable dilational structures. This contrasts with the other main sedimentary-hosted base-metal and polymetallic deposit types, which require unusual host rocks to act as chemical traps to precipitate mineralisation. There does not appear to be a favourable stratigraphic horizon for Cobar-style deposits.

Faults and shear zones as basin-scale conduits and mixing zones at deposit scale

Structures have played a crucial role in the genesis of Cobar-style deposits. Ductile high-strain zones. which have been interpreted as part of a thrust complex linked to shallowly dipping detachment (sole) structures, provided basin-scale conduits that tapped fluids from both within the basin and from underlying basement sources (Glen 1991, Robertson & Taylor 1987, Seccombe 1990). These channelways acted as zones of enhanced permeability, which drew in contrasting fluid types, perhaps episodically, throughout the inversion of the basin and, locally, at Peak, during extensional relaxation (Perkins et al. 1994). The structures also provided the necessary extensional geometry in otherwise compressional regimes that focussed the fluids into zones of non-laminar flow, where the conditions for fluid mixing and orebody formation were optimised.

Compressional reactivation of moderately to steeply dipping faults such as in the Cobar Basin requires supralithostatic fluid pressures. It is likely that this requires post-seismic flushing of fluids upwards from overpressured zones. At the commencement of basin inversion, it is envisaged that there was a transition from an extensional stress regime, with a high capacity to store fluids, to a compressional regime with comparatively low storage capacity. This led to preferential reactivation in the area of most intense overpressuring and rushing of fluids into pressure release zones, i.e. dilational structures.

This is illustrated by the distribution of alteration and mineralisation and quartz-vein textures in several Cobar deposits. For example, within the structure hosting the Elura orebodies, the zone of penetrative cleavage dies out above the northern orebodies. This has led to interpretation of the structure as a blind thrust (Lawrie 1988). The presence of such a structure near Elura is supported by seismic reflection profiles, which show the presence of a basin-floor discontinuity near the deposit (B. Goleby, pers com. 1997). Vein development and mineral precipitation were localised at the tip of this structure in an incipient anticline (Lawrie 1989a). Interconnectivity of the fluids in the high-strain zone hosting the multiple Elura orebodies is suggested by the similarity of metal grades at equivalent elevations in orebodies where vertical zonation in metal grades is marked (Lawrie 1989b, 1990b).

At Elura, early silicification in shales is primarily the result of crack-seal vein formation (de Roo 1989b), while in sandstones there is more pervasive silicification. Crack-seal veins were pervasively developed in the upper parts of the orebody before sulphidation and base-metal mineralisation, and more restricted with time and in the lower levels of the deposit. Sub-horizontal crack-seal veins are dominant in upper levels of the orebody (de Roo 1989b), indicating fluctuating fluid pressures and fault-valve activity (Cox et al. 1991, Sibson 1995), and repeated attainment of supralithostatic fluid pressures alternated with discharge episodes. The same crack-seal veins are not common at depth in stockwork veins.

Breccia veins, which are more indicative of catastrophic rupture and post-failure discharge, are common at depth. The low solubility of quartz and the extensive development of quartz veins, over several kilometres in strike length and, vertically, for more than one kilometre in some deposits, point to the involvement of significant fluid volumes. It is envisaged that formation of the Cobar orebodies involved episodic vertical migration of large fluid volumes along high-strain zones of relatively small displacement. The formation of massive zones of silicification up-dip of the tips of blind thrusts, at an early stage in evolution of the deposits, may effectively seal zones except in zones of maximum extension and structural breakthrough, and lead to formation of geochemically blind deposits with no obvious overlying alteration halo.

Other discontinuities in deeper level basement architecture may also play an important but less obvious role in the localisation of orebodies in the Cobar Basin. For example, many deposits around Cobar lie along strike from major NE-trending basin-scale faults (Fig. 3; Hinman 1992, Glen et al. 1996). These structures have been interpreted as transfer faults that were reactivated during basin inversion (Glen et al. 1996). A similar basement structure may localise the Elura orebodies.

At Peak and Elura, the doubly plunging anticlines that host the massive sulphide orebodies formed as a result of heterogeneous and high strains either along the plane of the HSZ/thrust or within more discrete high-strain volumes (Peak). Localisation of the Peak orebodies may, in part, be attributed to heterogeneous strain partitioning where rheology contrasts occur between thrust slices of rhyolite abutting sediments (Hinman 1991a, 1992, Perkins et al. 1994). However, the location of culminations at Elura cannot be related to known rheology contrasts or to the intersection of syn-HSZ folds with any pre-existing fold structures, e.g. the F1/F2 domes of de Roo (1989a). Mapping structural elements throughout the Elura deposit envelope shows maximum vertical dilation at the southernmost orebody and vertical extension and cleavage intensity dying out rapidly to the south, and much more gradually northwards (Fig. 6c,d).

A later transpressional shear zone, which cross-cuts and offsets the mineralised structure at Elura, appears to be an along-strike continuation of the prominent basin-scale Buckwaroon Fault, which has been interpreted as a reactivated transfer fault (Glen et al. 1996). It is speculated that the maximum extension seen in the southernmost orebody, and the similar but smaller scale features

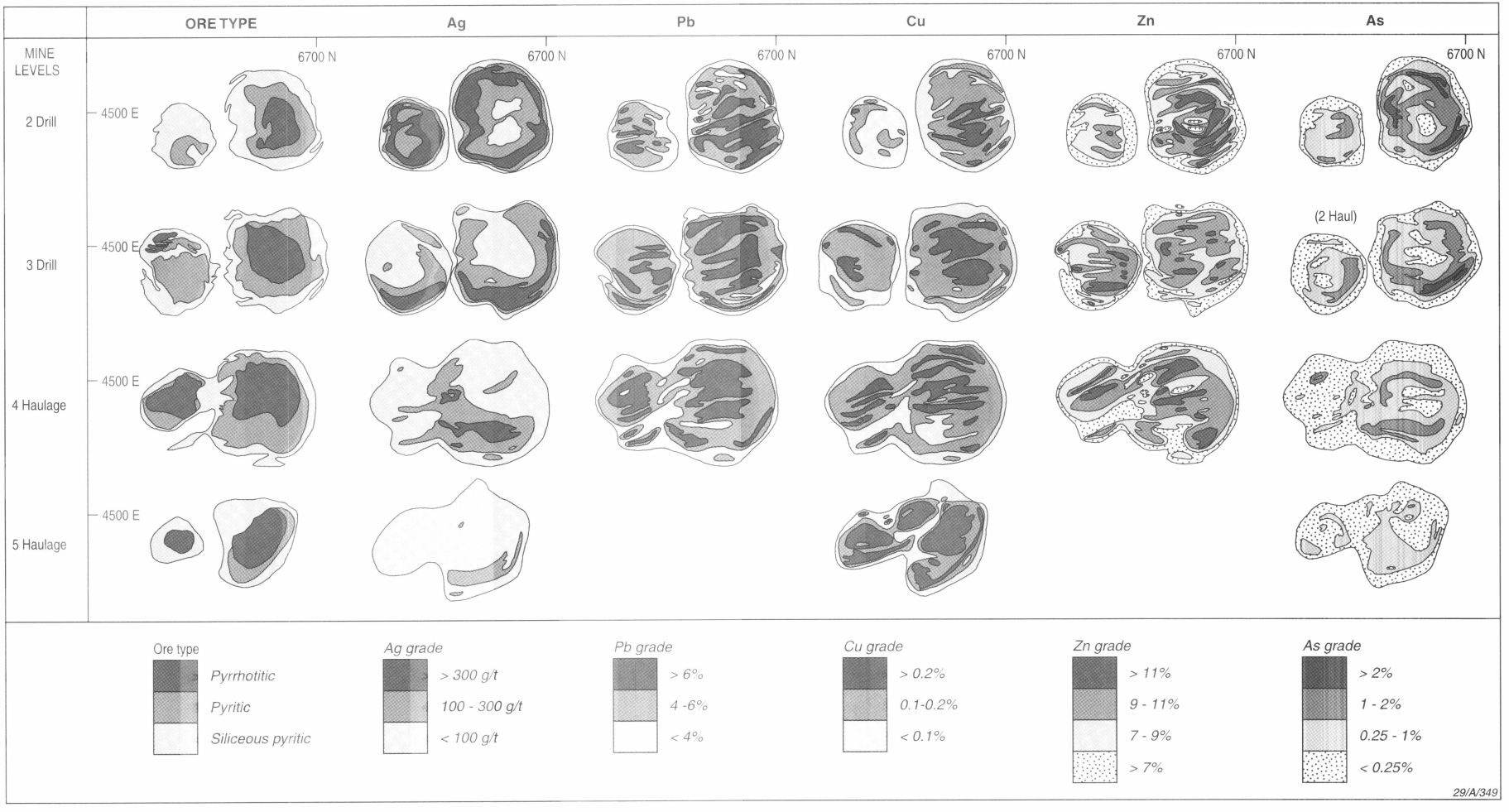

Figure 7. Contoured ore grades in the two southerly Elura ore bodies, for 2 drill, 3 drill, 4 haulage and 5 haulage levels. The plots are for Ag, Pb, Cu, Zn and As. After Lawrie (1990b).

associated with the northern orebodies, might coincide with underlying basement heterogeneities associated with an extension to, or splays at the termination of, the Buckwaroon Fault.

Fluids

A complex pre-, syn- and post-mineralisation fluid history is preserved within and near the Cobar deposits. There is evidence of episodic reactivation of key mineralised structures, some of which may have originated as syn-sedimentary faults (Glen 1991). These were reactivated as compressional thrust faults, and appear to have acted as channelways for the expulsion of fluids episodically throughout basin inversion. Resolving the complexities of these fluid components is important for establishing genetic models and in assessing the use of alteration haloes in exploration for analogous deposits.

Cryptic alteration haloes characterised by alkali element and base-metal depletion zones occur in the host rock adjacent to several of the Cobar deposits (Robertson & Taylor 1987, Schmidt 1980). These depletion haloes are considerably more extensive than the high-strain zones of penetrative cleavage development and, in the absence of cleavage (fracture) permeability, it has been suggested that formation of these vertically extensive zones may be related to flow of acidic basinal fluids that created their own secondary permeability channels above or near faults at an early stage in the expulsion of fluids from the basin (Robertson & Taylor 1987). Robertson & Taylor (1987) suggested that dissolution of detrital minerals and stripping of base metals was accomplished by basinal fluids containing organic acids (carboxylic and/or acetic acids) formed as a result of maturation of kerogens at depth within the basement. This interpretation is supported by paragenetic evidence, vitrinite reflectance profiles, and fluid inclusion data from quartz veins in the deposits which show that oilfield brines were generated in the basin and expelled through the high-strain zones at a later stage. A similar pre-mineralisation, reduced connate origin has been proposed for fluids that deposited pyrrhotite haloes updip to (and overprinted by) mineralisation at the Peak deposit (Hinman 1992).

The earliest measurable fluid-inclusion data from quartz veins in the deposits reveal that, even at a relatively early paragenetic stage in the evolution of the structures, there was complex fluid flow and interaction. In both the Peak and Elura deposits, two dissimilar fluids, with different homogenisation temperatures and compositions, are thought to be present in varying proportions through time and have mixed at the site of orebody formation. One fluid has a high temperature (T_h >350°C at Peak; T_h >250°C at Elura), with low salinity, contains CO_2, and is either relatively oxidised (near the pyrite–magnetite buffer; Hinman 1992), or had a low H_2S activity. This fluid has been interpreted to be of basement origin, with a metamorphic origin (Seccombe 1990), or either metamorphic or magmatic origin proposed (Hinman 1992).

A second fluid, present at both Peak and Elura, is relatively reduced and becomes progressively hotter and more saline through the paragenetic sequence of both deposits (Hinman 1991a, b, 1992, Lawrie 1990c, 1991b). At Elura, the earliest trapped fluid contains n-alkanes and is essentially an oilfield brine (Lawrie 1991b). An ethane-bearing fluid, interpreted to be a more evolved variant of this brine, is observed in the paragenesis immediately prior to mineralisation (Lawrie 1990c). A progressively more saline (up to 15% wt. equiv. NaCl), hotter (T_h up to 370°C), methane-rich fluid is present in later syn-mineralisation paragenetic stages (Lawrie 1990, 1991, Seccombe 1990). At the Peak deposit, an analogous methane-rich fluid similarly becomes progressively hotter and more saline (up to 12.5% wt equiv. NaCl; Hinman 1992, Jiang & Seccombe 1995), and hotter through the paragenesis (T_h 150–350°C, Hinman 1992). The progressive (or episodic) shift to less complex n-alkane content with increasing salinity and temperature through time is consistent with derivation of these relatively reduced hydrocarbon-bearing fluids from a basinal (connate) source that evolved with an increase in the thermal maturation of basin sediments during diagenesis.

In both the Peak and Elura deposits, mixing of these basinal and basement-derived fluids appears to play an important role in orebody formation. Precipitation of metals in these dilational sites is most likely due to the mixing of these two fluids, which have contrasting temperatures, redox conditions and salinities (Lawrie 1990c, 1991a, Hinman 1991a,b, 1992). Although fluid inclusions record heterogeneous entrapment, the bulk compositions support mixing and cannot be rationalised by unmixing or boiling (Hinman 1992). Differences in metal ratios between the deposits are most likely a reflection of different relative contributions from the two fluids. A more basinal signature is characteristic of within-basin deposits, such as Elura, that are also higher in the stratigraphic sequence, whereas deposits such as Peak are in an area with a greater proportion of acid volcanics at depth, and are physically closer to potential basement fluid sources. At Elura, the ore paragenesis is initially Zn-rich, then Pb–Zn–Ag dominant, and becomes progressively more polymetallic and Cu-rich with an increase in temperature of the hydrothermal system through time. Mixing with locally derived, lower temperature basinal fluids is unlikely to have provided a major fluid input into the deposits, owing to the lithified nature of the host rocks and the lack of permeability outside the high-strain zones.

Also of importance is the timing of introduction of metals with respect to vein development and remobilisation of ore during progressive deformation, synchronous with orebody formation. At Elura, preliminary geochemical modelling of metal zoning is explained in terms of mixing of fluids, with precipitation also considered to be a function of temperature (cooling) gradients towards orebody margins. Although the data for the northern Elura orebodies are more limited, similar patterns of metal distribution are generally noted. The similarity in metal values with depth in all seven discrete orebodies is considered to indicate that common physico-chemical gradients applied throughout the high-strain zone hosting mineralisation. Metal zoning in the other deposits, such as Peak, is equally or more complex. The presence of magnetite indicates that the orebodies around Cobar formed from fluids that were more oxidised, hotter, or had lower H_2S activity compared with deposits further north.

Heat flow environment

An important component of the genetic model for formation of the Cobar deposits is regional heating of the basin and the timing of that event synchronous with inversion. Heating on a regional scale, together with subsequent cooling, is often synchronous with basin inversion events (Green et al. 1995). It is commonly a function of regional burial followed by uplift and erosion. Telescoping of thermal gradients in inversion zones is common as rocks are uplifted and exposed to a cooler environment, and hotter fluids are brought from depth.

The formation of the Cobar deposits links the physical effects of basin inversion, (expressed as brittle–ductile deformation in restricted high-strain zones) with the telescoping of geotherms and mixing of fluids from within the basin with those derived externally from the basement (Lawrie 1991, Hinman 1992). It is suggested that mineralisation began while host rocks (at deeper levels) were in the methane generation window (Lawrie 1990b). Illite crystallinity (Brill 1988b) and vitrinite reflectance data (Schmidt 1980) from lower strain domains adjacent to some of the deposits indicate that, outside major fluid channels, the basin was heated to upper diagenetic conditions. Basin inversion synchronous with ongoing sedimentation or shortly after cessation of deposition (pre-Mulga Downs Group) is supported by Pb isotope data (Jiang & Seccombe 1995, Hinman 1992).

Structures that host mineralisation were episodic fluid conduits over a considerable time, with fluids evolving from oilfield brines (and possibly earlier diagenetic fluids) to later hotter, methane-bearing connate fluids, preserved in several

deposits (Lawrie 1990b, 1991, Hinman 1992). Magmatic input at the McKinnons Au deposit is suggested by the presence of an advanced argillic alteration assemblage (Bywater et al. 1996).

Metal, sulphur and fluid sources

The origin of the metals themselves is potentially crucial to understanding the relative roles of basinal and basement-derived fluids, and in formulating exploration models. Hinman (1994) has argued that the metals were derived from different sources, with Au, Cu, and some of the Pb, Zn and Ag sourced from the basement-derived fluids, and the basinal fluid supplying most of the Pb, Zn and Ag. Glen (1991) related differences in metal ratios and derived fluids to differences in thrust geometry.

Sulphur isotope data suggest that sulphur within the orebodies is sourced from within host metasedimentary Cobar Supergroup sediments (Seccombe 1990). Lead isotope data from orebody sulphides point to a mixed source, with both basinal and basement components evident (Fig. 8a, b). The more Pb–Zn end member of the mineralisation spectrum, such as the Elura deposit, appears to represent basinal dominance, whereas Cu–Au is basement–metamorphic dominant, although still mixed (Hinman 1992).

The occurrence of a greater proportion of volcanics at depth in the southern half of the basin may play an important role in the sourcing and transportation of different metals in the basin (Hinman 1991a, b, 1992, Lawrie 1991a) and may partly explain the regional zoning in metals noted in the basin.

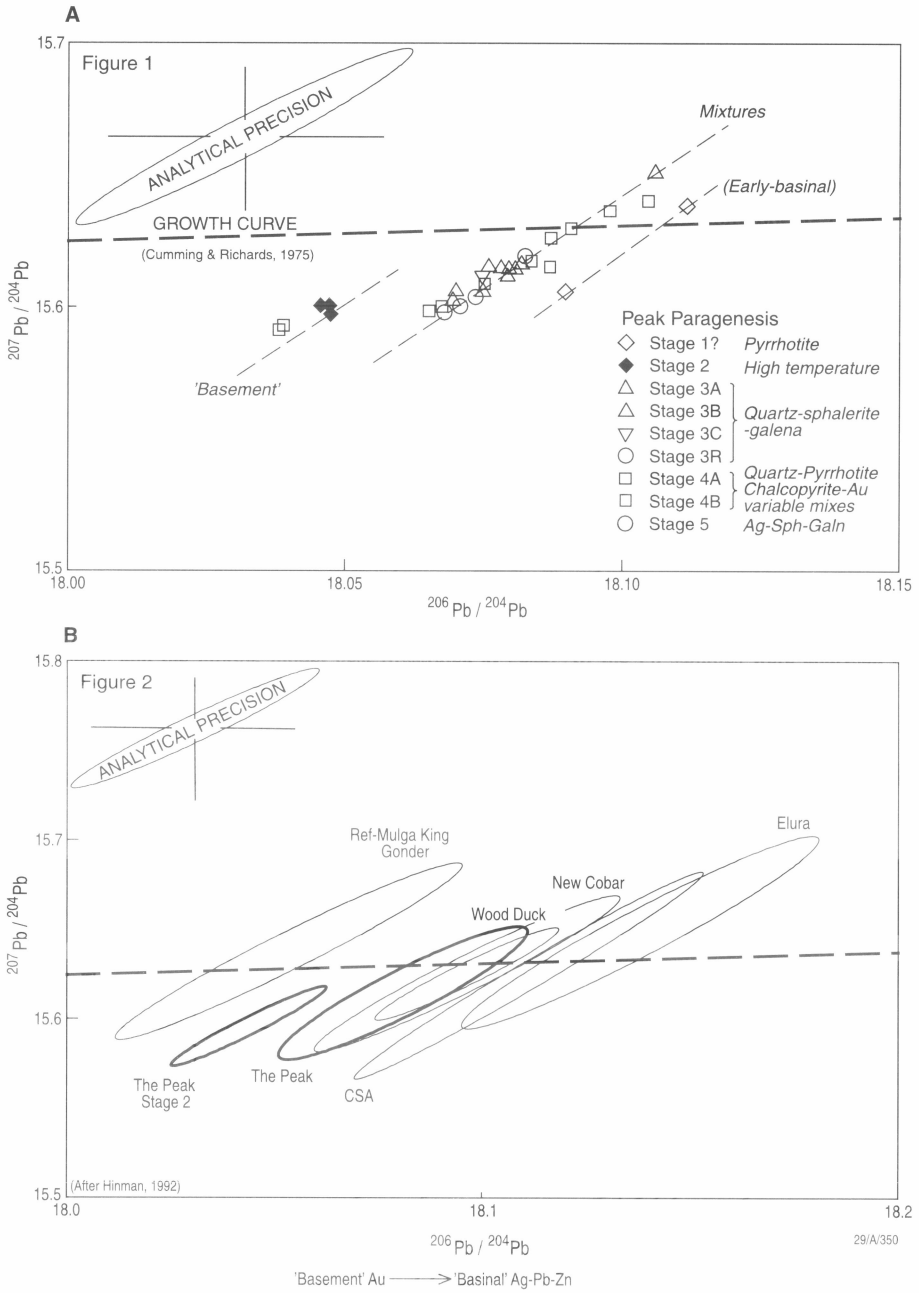

Figure 8. (a) Pb isotope data for the Peak deposit, plotted on a ^{207}Pb–^{206}Pb with samples identified by their paragenetic stage. Given the analytical precision, the data fall into three groupings. The most radiogenic group (Stage 1) is from pyrrhotised sediments up-dip of the main mineralisation, the high temperature pyritic Stage 2 and some Stage 4b samples form a distinctive low radiogenic group. The bulk of the mineralisation falls within an intermediate radiogenic group. The data suggest that two Pb sources were present within the mineralising system and that the bulk of the mineralisation represents mixtures of the two Pb sources. **(b) Pb data from the Peak and other Cobar deposits.** The Pb data indicate that the base metal-rich systems are dominated by the more radiogenic Pb (e.g. Elura, CSA), while the Au-rich systems (e.g. Peak, Mulga King at Mt Boppy), are dominated by the less radiogenic Pb. The data support the presence of two source components and the mixing model best illustrated at Peak. All the Pb samples were analysed by Graham Carr of SIROTOPE, and his permission to publish the Pb data is acknowledged.

Timing of deposit formation

Most of the Cobar deposits appear to have formed synchronously with basin inversion, with channelling of fluids in high-strain zones of penetrative cleavage. Whole-rock Ar/Ar dating of regional cleavage dates the inversion event at 395–400 Ma, and it is likely that the Cobar deposits formed within this range (Glen et al. 1992a,b). However, two distinct mineralising events are recognised at Peak (Perkins et al. 1994). These are (Ag)–Pb–Zn–Cu–Au mineralisation, which is syn-inversion and penetrative cleavage formation (e.g. 401 ± 1.1 Ma at Peak); and later replacement Ag–Pb–Zn mineralisation, which formed during extensional relaxation of earlier contractional structures (384 ± 1.4 Ma at Peak).

Summary

The polymetallic deposits of the Cobar Basin are complex orebodies that formed from the mixing of contrasting fluid components derived from sources outside and within the Cobar Basin. Essentially, the formation of these Early Devonian deposits overlaps with basin inversion (Glen et al. 1992a,b, Perkins et al. 1994), with one additional style of mineralisation coinciding with a much later period of basin extension (Perkins et al. 1994). Faults and shear zones provide the necessary fluid channels and dilational zones, with high-strain volumes

and zones providing the permeability within which fluids were focussed and mixed, and where orebodies thus formed (Fig. 2).

Alternative theories for the genesis of the Cobar deposits have included hydrothermal replacement models (Andrews 1913, Sullivan 1951, Mullholland & Rayner 1961); sediment-hosted models (Brooke 1975, Gilligan & Suppel 1978, Sangster 1979, Marshall et al. 1981); and locally remobilised sediment-hosted models (Marshall & Gilligan 1993). None of these studies appears to have considered or fully integrated the available structural and microstructural data essential for constraining the paragenetic development of these complex orebodies. In addition to the involvement of basinal (connate) and basement (metamorphic) fluids, some evidence suggests the possibility of meteoric and possibly even an igneous component in the genesis of some of the deposits in the Cobar Basin (Bywater et al. 1996, Jiang & Seccombe 1995, Jiang et al. 1995a,b). Hinman (1994) has proposed that the late-stage, de-silicifying replacment mineralisation at Peak may have formed as a consequence of a down-flow of meteoric water.

Comparison with other sediment-hosted base-metal and polymetallic deposits

The Cobar deposits differ significantly from other types of polymetallic base and precious-metal deposits, such as SEDEX, MVT, and Tennant Creek, although there are some similarities in individual characteristics within specific deposits.

A key difference between the Cobar style and SEDEX deposit types is in the timing and method of fluid migration through host rocks. Most Cobar orebodies formed from fluids that utilised fracture permeability within brittle–ductile shear zones formed during basin inversion. In contrast, SEDEX deposits are generally thought to have utilised bedding porosity and permeability channels and the fluids from which they form are thought to have been expelled from basins in response to buoyancy-driven fluid flow (Large 1995).

Another significant difference lies in fluid composition. Basinal brines are recognised as the dominant or sole fluid component in other base-metal SEDEX deposits (Large 1995). This contrasts with the Cobar deposits, in which more than one fluid component is recognised. Mixing of these fluid components is an important factor in orebody formation in Cobar orebodies. Also, unusual host-rock compositions do not appear to play an important role in ore precipitation in the Cobar deposits. This contrasts with stratiform shale-hosted base-metal deposits, which require reduced sedimentary host rocks, MVT and Irish-style base-metal deposits, which are hosted by carbonate rocks, and the Broken Hill deposits, which require oxidised host rocks (Large 1995).

In comparison with MVT deposits, the mineralising fluids responsible for formation of the Cobar orebodies differ, in having a greater temperature range and overall much higher temperatures for the Cu–Au end of the spectrum and lower fluid salinities (Kesler et al. 1995). One consequence of this is that the fluids that formed the Cobar deposits were capable of the transport and deposition of more varied metals, particularly higher Cu and Au (Sverjensky 1986).

MVT deposits are generally formed during expulsion of saline connate waters and hydrocarbons prior to lithification, with high intergranular permeabilities and shale membrane transport important for fluid migration. It seems more likely that the Cobar deposits represent a deposit type formed intermediate in time between classic MVT deposits and solely metamorphic-fluid sourced deposits. This model is consistent with an increase in geothermal gradients in the Cobar Basin at the onset of basin inversion.

Similarities between Cobar deposits and Tennant Creek orebodies include similarities in pipe-like orebody geometry, the multi-stage parageneses, and the proposed sourcing of fluids from basinal (connate) and basement (+ igneous) fluid sources. The most significant differences would appear to lie in the much more oxidised host rocks and (basinal) fluid conditions at Tennant Creek (Zaw et al. 1994). These differences may help explain differences in metal ratios and mineralogy between Cobar and Tennant Creek deposits (Ferenczi 1994).

Exploration for Cobar-style deposits

The geophysical and geochemical criteria established for the known Cobar deposits are summarised in the introductory pages. From these data, it is evident that identification of favourable structural geometry within high-strain zones is crucial as a first step in target generation, particularly in areas where orebodies are buried and have not been affected by near-surface weathering. Delineation of possible host structures requires structural mapping in subcropping areas, combined with aeromagnetic and gravity datasets to identify buried structures and basement heterogeneities.

Other techniques, such as seismic reflection profiling, are of use in identifying major structures, but delineation of deposit-scale faults is hampered by lack of velocity contrast in homogeneous basin sediments, although higher resolution seismic reflection profiling may provide information on near-surface structures. Aeromagnetic data can also potentially identify the point source anomalies of some deposits (Emerson 1980), with relatively weak pyrrhotite anomalies in some deposits (eg Elura, Peak) and magnetite with some Cu–Au deposits (e.g. Chesney, Great Cobar).

Exploration at depth near existing deposits is assisted by collection of oriented structural and bedding data from drill core (Lawrie 1988, Hinman 1991a). At Elura, this permitted delineation of the northern orebodies (Lawrie 1988, 1990a), and led to recognition of offsetting shear zones south of the main deposits. At Peak, structural analysis of drill core assisted with resolving the geometry of complex orebodies and indicated that anomalous structure provides a much larger drilling target than any anomalous geochemistry (Hinman 1992). The blind nature of the structural geometry hosting the northern Elura orebodies demonstrates that structural mapping by itself may not necessarily locate analogous deposits. Structural studies have been augmented by the use of down-hole magnetics and RIM technology in near-mine exploration at the existing mines.

A range of geochemical techniques shows the presence of significant geochemical anomalies (Dunlop et al. 1995, Cohen et al. 1996); however, further work appears to be required to understand the dispersion of geochemical anomalies in surficial maghemite lags and in subsurface regolith (D. Gibson, pers comm. 1997). The complexity of the regolith in the Cobar Basin most likely adds to concealment of any near-surface deposits (Leah 1996).

Within and marginal to the basin, there is the potential for other deposit styles sourced from the same fluid components present in the Cobar deposits. Examples may include base-metal mineralisation hosted by marginal carbonate sequences, and Au–Cu deposits in reduced clastic sequences within the adjacent basement terrane (Wagga High). These targets are more likely to be dependent on precipitation in favourable host rocks. The latter model is also dependent on availability of basement-derived fluids and continuity of major structures, such as the Rookery Fault.

Elsewhere, exploration for Cobar-style deposits should be focussed on reduced sedimentary basins with similar burial and inversion histories. These include high heat flow intracratonic basins that inverted while source rocks were in the gas generation window and inversion zones within some intracratonic rift basins. In some scenarios, foreland basins might also be prospective for similar deposits.

Acknowledgments

The authors wish to thank E.Z./N.B.H./Pasminco (KL) and Cobar Mine Proprietary Limited and Peak Gold Mines (MCH)

for supporting the studies of the Elura and Peak deposits respectively. Graham Carr of CSIRO generously carried out the Pb work for MCH's study and is thanked for allowing its delayed publication here. We would also like to thank David Huston and Dick Glen for reviewing the manuscript, and Lana Murray for drafting the diagrams.

References

Andrews, E.C., 1913. Report on the Cobar Copper and Gold Field, Part 1. Mineral Resources, No. 17. New South Wales Department of Mines, Sydney.

Binns, R.A. & Appleyard, E.C., 1986. Wallrock alteration at the Western System of the C.S.A mine, Cobar, New South Wales, Australia. Applied Geochemistry, 1, 211–225.

Brill, B.A., 1988a, The geochemistry and genesis of the CSA Cu–Pb–Zn deposit, NSW, Australia: Unpublished Ph.D. thesis, Newcastle University, Australia.

Brill, B.A., 1988b. Illite crystallinity, b (sub 0) and Si content of K-white mica as indicators of metamorphic conditions in low-grade metamorphic rocks at Cobar, New South Wales. Australian Journal of Earth Sciences, 35, 295–302.

Brill, B.A., 1989. Deformation and recrystallisation microstructures in deformed ores from the CSA mine, Cobar, N.S.W., Australia. Journal of Structural Geology, 11, 591–601.

Brill, B.A., 1989. Deformation and recrystallisation microstructures in deformed ores from the CSA Mine, N.S.W., Australia; reply. Journal of Structural Geology, 13, 119–120.

Brooke, W.J.L., 1975. Cobar mining field. Australasian Institute of Mining and Metallurgy, Monograph 5, 683–694.

Bywater, A., Johnston, C., Hall, C.R., Wallace Bell, P. & Elliot, S.M., 1996. In: Cook, W.G. et al. (editors), The Cobar mineral field—a 1996 perspective. Australasian Institute of Mining and Metallurgy, Spectrum Series, 3/96, 279–292.

Clark, D.A. & Tonkin, C., 1994. Magnetic anomalies due to pyrrhotite: examples from the Cobar area, N.S.W., Australia. Journal of Applied Geophysics, 32, 11–32.

Cohen, D.R., Rutherford, N.F., Dunlop, A.C. & Alipour, S., 1996. Geochemical exploration in the Cobar region. In: Cook, W.G., Ford, A.J.H., McDermott, J.J., Standish, P.N., Stegman, C.L. & Stegman, T.M. (editors), The Cobar mineral field—a 1996 perspective. Australasian Institute of Mining and Metallurgy, Spectrum Series, 3/96, 125–156.

de Roo, J. A., 1989a. The Elura Ag–Pb–Zn Mine in Australia—ore genesis in a slate belt by syndeformational metasomatism along hydrothermal fluid conduits. Economic Geology, 84, 256–278.

de Roo, J. A., 1989b. Mass transfer and preferred orientation development during extensional microcracking in slate-belt folds, Elura Mine, Australia. Journal of Metamorphic Geology, 7, 311–322.

Drummond, B.J., Glen, R.A., Goleby, B.R., Wake-Dyster, K.D. & Palmer, D., 1992. Deep seismic of the Cobar Basin II: a ramp basin controlled by mid-crustal detachment. Geological Society of Australia, Abstracts, 32, 44.

Dunlop, A.C., Atherden, P.R. & Govett, G.J.S., 1983, Lead distribution in drainage channels about the Elura zinc–lead-silver deposit, Cobar, New South Wales. Journal of Geochemical Exploration, 18, 195–204.

Emerson, D.W. (editor), 1980. The geophysics of the Elura orebody, Cobar, New South Wales. Australian Society of Exploration Geophysicists, Sydney, 205 pp.

Ferenczi, P., 1994. Are Tennant Creek style ironstone-related gold–copper–bismuth deposits unique? A review of available data and a comparison with possible analogous deposits. In: Hallenstein, C.P. (editor), 1994 AusIMM annual conference, Australian mining looks north; the challenges and choices. Australasian Institute of Mining and Metallurgy, Publication Series, 5/94, 171–177.

Gilligan, L & Byrnes, J.G., 1995. Cobar 1:250,000 metallogenic Map SH/55-14: metallogenic study and mineral deposit data sheets. Geological Survey of New South Wales, Sydney. 240 pp.

Gilligan, L.B & Suppel, D.W., 1978. Mineral deposits in the Cobar Supergroup and their structural setting. New South Wales Geological Survey, Quarterly Notes, 33, 15–22.

Glen, R.A., 1985. Basement control on the deformation of cover basins: an example from the Cobar district in the Lachlan Fold Belt, Australia. Journal of Structural Geology, 7, 301–315.

Glen, R.A., 1987. Copper- and gold-rich deposits in deformed turbidites at Cobar, Australia: their structural control and hydrothermal origin. Economic Geology, 82, 124–141.

Glen, R.A., 1990. Formation and inversion of transtensional basins in the western part of the Lachlan fold belt, Australia, with emphasis on the Cobar Basin. Journal of Structural Geology, 12, 601–620.

Glen, R.A., 1991. Inverted transtensional basin setting for gold and copper and base metal deposits at Cobar, New South Wales. BMR. Journal of Australian Geology & Geophysics, 12, 13–24.

Glen, R.A., 1995. Thrusts and thrust-associated mineralisation in the Lachlan Orogen. Economic Geology, 90, 1402–1429.

Glen, R.A., Dallmeyer, R.D. & Black, L.P., 1992a. Isotopic dating of basin inversion—the Palaeozoic Cobar Basin, Lachlan Orogen, Australia. Tectonophysics, 214, 249–268.

Glen, R.A., Scheibner, E. & VandenBerg, A.H.M., 1992b. Paleozoic intraplate escape tectonics in Gondwanaland and major strike-slip duplication in the Lachlan orogen of southeastern Australia. Geology, 20. 795–798.

Glen, R.A., Drummond, B.J., Goleby, B.R., Palmer, D. & Wake-Dyster, K.D., 1994. Structure of the Cobar Basin, New South Wales, based on seismic reflection profiling. Australian Journal of Earth Sciences, 41. 341–352.

Glen, R.A., Clare, A. & Spencer, R., 1996. Extrapolating the Cobar Basin model to the regional scale: Devonian basin formation and inversion in western New South Wales. In: Cook, W.G., Ford, A.J.H., McDermott, J.J., Standish, P.N., Stegman, C.L. & Stegman, T.M. (editors), The Cobar mineral field—a 1996 perspective. Australasian Institute of Mining and Metallurgy, Spectrum Series, 3/96, 43–84.

Green, P.F., Duddy, I.R. & Bray, R.J., 1995. Applications of thermal history reconstruction in inverted basins. In: Buchanan, J.G & Buchanan, P.G. (editors), Basin inversion. Geological Society Special Publication 88, 149–166.

Hinman, M.C., 1989, Syntectonic precious and base metal mineralization controlled by deformation partitioning during an Early Devonian orogeny at Peak, Cobar, N.S.W. Geological Society of Australia, Specialist Group on Tectonics and Structural Geology, Conference Proceedings, Geological Society of Australia, Abstracts, 24, 71–72.

Hinman, M.C., 1991a. Speculation in chaos at Cobar—the Peak experience. In: Lawrie, H.F.C. (editor). Base metals symposium. James Cook University, Economic Geology Research Unit Contribution 38, 144–166.

Hinman, M.C., 1991b. Paragenesis of a syn to post cleavage, multistage, base and precious metal ore system at Peak, Cobar, NSW. Bureau of Mineral Resources, Australia, Record 1990/95, 33–34.

Hinman, M.C., 1992. The structure and geochemical genesis of of the Peak base and precious metal deposit, Cobar, New South Wales. Unpublished Ph.D. thesis, James Cook University of North Queensland.

Hinman, M.C. & Scott, A., 1990. The geology of the Peak deposit, Cobar. In: Hughes, F.E., (editor), Geology of the mineral deposits of Australia and Papua New Guinea. Australasian Institute of Mining and Metallurgy, Monograph 14, 1345–1351.

Hone, I.G. & Gidley, P.R., 1986. Investigation of the characteristics and sources of the Magnetic Ridge magnetic anomaly,

Cobar, NSW. Bureau of Mineral Resources, Australia, Report 248, 26 pp.

Jeffrey, S. & Thomson, S., 1996. RIM technology and the CSA copper mine, Cobar, NSW—a joint research and development project for a base metal mine. In: Cook, W.G., Ford, A.J.H., McDermott, J.J., Standish, P.N., Stegman, C.L. & Stegman, T.M. (editors), The Cobar mineral field—a 1996 perspective. Australasian Institute of Mining and Metallurgy, Spectrum Series, 3/96.

Jiang, Z. & Seccombe, P.K., 1994. Fluid inclusion geochemical study of the Peak Gold Deposit, Cobar, NSW. Geological Society of Australia, Abstracts, 37, 198.

Jiang, Z. & Seccombe, P.K., 1995. Pb and Sr isotope characteristics of mineralisation and host rocks and new ages for igneous activity and mineralisation at Peak mine, Cobar, NSW. Centre for Isotope Studies, Report 1993–94, 76–81.

Jiang, Z., Seccombe, P.K., Andrew, A.S., Todd, A.J. & Luo, Z., 1995a. Oxygen and hydrogen isotope study at the Peak mine, Cobar, N.S.W. Centre for Isotope Studies, Report 1993–94, 71–75.

Jiang, Z., Seccombe, P.K., Andrew, A.S. & Todd, A.J., 1995b. Stable isotope signature of the Chesney Cu–Au vein deposit, Cobar, NSW. Centre for Isotope Studies, Report 1993–94, 82–87.

Kesler, S.E., Appold, M.S., Martini, A.M., Walter, L.M., Huston, T.J. & Kyle, J.R., 1995. Na–Cl–Br systematics of mineralising brines in Mississippi Valley-type deposits. Geology, 23, 641–644.

Large, R.R., 1995. Key features and ore deposit models for sediment-hosted Pb–Zn–Ag deposits. In: Large, R.R. (editor), Ore forming processes and ore deposit models. Vol. 3, Sediment-hosted Pb–Zn–Ag deposits, 1–23. Unpublished Short Course for Australian Geological Survey Organisation.

Lawrie, K.C., 1988. Structural controls on the northern orebodies at the Elura Mine. Unpublished report to E.Z. Ltd.

Lawrie, K,C., 1989a. Structural prediction of geophysically and geochemically blind orebodies at the Elura Mine, N.S.W. Unpublished report to N.B.H. Ltd.

Lawrie, K. C., 1989b. Structural controls and prediction of syntectonic massive sulphide orebodies at Elura Mine, Cobar, N.S.W. Geological Society of Australia, Specialist Group on Economic Geology, Cobar Field Meeting Workshop, 4 pp. (extended abstract).

Lawrie, K.C. 1990a. Exploration for syntectonic massive sulphide deposits based on structural and microstructural analysis of drillcore. Geological Society of Australia, Abstracts, 25, 179.

Lawrie, K.C. 1990b. Metal zoning and ore paragenesis in the Elura orebodies, N.S.W. Unpublished report to N.B.H. Ltd.

Lawrie, K.C., 1990c. Ore paragenesis, fluid history, and alteration paragenesis and halos in the main and northern orebodies at Elura, N.S.W. Unpublished report to N.B.H. Ltd.

Lawrie, K.C., 1991a. The Cobar base metal deposits, N.S.W. In Lawrie, H.F.C. (editor), Base metals symposium. James Cook University, Economic Geology Research Unit, Contribution 38, 137–143.

Lawrie, K.C., 1991b. Metal zoning and fluids in the Elura orebodies, N.S.W.: implications for formation of syntectonic massive sulphide orebodies. Bureau of Mineral Resources, Australia, Record 1990/95, 52 (abstract).

Leah, P.A., 1996. Relict laterite weathering profiles in the Cobar District, NSW. In: Cook, W.G., Ford, A.J.H., McDermott, J.J., Standish, P.N., Stegman, C.L. & Stegman, T.M. (editors), The Cobar mineral field—a 1996 perspective. Australasian Institute of Mining and Metallurgy, Spectrum Series, 3/96, 157–178.

Marshall, B., 1989. Deformation and recrystallisation microstructures in deformed ores from the CSA Mine, N.S.W., Australia; discussion. Journal of Structural Geology, 13, 117–118.

Marshall, B. & Gilligan, L.B., 1993. Remobilistion, syn-tectonic processes and massive sulphide deposits. Ore Geology Reviews, 8, 39–64.

Marshall, B., Sangameshwar, S.R., O'Connor, D.P.H., Sun, S-S. & Bouffler, M., 1981. Genetic aspects of the C.S.A. and Q.T.S. mineralisations, Cobar, N.S.W. Geological Society of Australia, Abstracts, 3, 4.

McDermott, J, Smith, C. & Jeffrey, J., 1996. CSA Geology. In: Cook, W.G., Ford, A.J.H., McDermott, J.J., Standish, P.N., Stegman, C.L. & Stegman, T.M. (editors), The Cobar mineral field—a 1996 perspective. Australasian Institute of Mining and Metallurgy, Spectrum Series, 3/96, 197–214.

Mulholland, C. St. J. & Rayner, E.O., 1961. The gold–copper deposits of Cobar, New South Wales: Central Section (Great Cobar to New Occidental): New South Wales Department of Mines, Technical Report 6 for 1958, 28–49.

O'Conner, D.P.H., 1980, Evidence of an exhalative origin for deposits of the Cobar district, NSW; discussion: BMR Journal of Australian Geology & Geophysics, 5, 70–72.

Perkins, C., Hinman, M.C. & Walshe, J.L., 1994. Timing of mineralisation and deformation, Peak Au mine, Cobar, New South Wales. Australian Journal of Earth Sciences, 41, 509–522.

Phillips, G. N. & Powell, R., 1993. Link between gold provinces. Economic Geology, 88, 1084–1098.

Pogson, D. J. & Hilyard, D., 1981. Results of isotopic age dating related to Geological Survey of New South Wales investigations, 1974–1978. Geological Survey of New South Wales, Records, 20, 251–273.

Robertson, I. G., 1974. Environmental features and petrogenesis of the mineral zones of Cobar, N.S.W. Unpublished Ph.D. thesis, University of New England, 445 pp.

Robertson, I. D. M. & Taylor, G. F., 1987. Depletion haloes in fresh rocks surrounding the Cobar ore bodies, NSW, Australia: implications for exploration and ore genesis. Journal of Geochemical Exploration, 27, 77–101.

Russell, R.T. & Lewis, B.R., 1965. Gold and copper deposits of the Cobar district: Geology of Australian ore deposits: Proceedings of Eighth Commonwealth Mining and Metallurgical Congress, Melbourne, 1, 411–419.

Sangster, D.F., 1979. Evidence of exhalative origin for deposits of the Cobar district, New South Wales. BMR Journal of Australian Geology & Geophysics, 4, 15–24.

Saxby, J.D., 1981. Organic matter in ancient ores and sediments. BMR Journal of Australian Geology & Geophysics, 6, 287–291.

Schmidt, B.L., 1980. Geology of the Elura Ag–Pb–Zn deposit, Cobar District, N.S.W. Unpublished M.Sc. thesis, Australian National University.

Schmidt, B.L., 1990, Elura zinc–lead–silver mine, Cobar. In: Hughes, F.E. (editor), Geology of the mineral deposits of Australia and Papua New Guinea, Australasian Institute of Mining and Metallurgy, Monograph 14, 1329–1336.

Schneider, M.N. & Emerson, D.W., 1980. Physical properties of the Elura prospect, Cobar, NSW. Australian Society of Exploration Geophysicists, Bulletin, 11, 184–185.

Scott, A.K. & Phillips, K.G., 1990. C.S.A. copper–lead–zinc deposit, Cobar. In: Hughes, F.E. (editor), Geology of the mineral deposits of Australia and Papua New Guinea, Australasian Institute of Mining and Metallurgy, Monograph 14, 1337–1343.

Seccombe, P., 1990. Fluid inclusion and sulphur isotope evidence for syntectonic mineralisation at the Elura Mine, southeastern Australia. Mineralium Deposita, 25, 304–313.

Sibson, R.H., 1995. Selective fault reactivation during basin inversion: potential for fluid redistribution through fault-valve action. In Buchanan, J.G. & Buchanan, P.G. (editors), Basin inversion. Geological Society Special Publication 88, 3–20.

Smith, J.V., 1992. Experimental kinematic analysis of en ech-

elon structures in relation to the Cobar Basin, Lachlan Fold Belt. Tectonophysics, 214, 269–276.

Spencer, R.A., Tyne, E.D., Daggar, D.H. & Leys, M.T.C., 1992. Gravity map of New South Wales. Geological Survey of New South Wales, Sydney.

Stegman, C.L., 1998. It's all a matter of competency—exploring in the Cobar gold field, NSW. Australian Institute of Geoscientists, Bulletin 23, 75–82.

Stegman, C.L. & Pocock, J.A., 1996. The Cobar gold field—a geological perspective. In: Cook, W.G., Ford, A.J.H., McDermott, J.J., Standish, P.N., Stegman, C.L. & Stegman, T.M. (editors), The Cobar mineral field—a 1996 perspective. Australasian Institute of Mining and Metallurgy, Spectrum Series, 3/96, 229–264.

Stegman, C.L. & Stegman, T.M., 1996. History of mining in the Cobar region. In: Cook, W.G., Ford, A.J.H., McDermott, J.J., Standish, P.N., Stegman, C.L. & Stegman, T.M. (editors), The Cobar mineral field—a 1996 perspective. Australasian Institute of Mining and Metallurgy, Spectrum Series, 3/96, 3–42.

Sullivan, C.J., 1947. The geology of the Cobar mineral field and its bearings on prospecting. Bureau of Mineral Resources, Australia, Record 1947/74.

Sullivan, C.J., 1951. Geology of New Occidental, New Cobar and Chesney Mines, Cobar, New South Wales. Bureau of Mineral Resources, Australia, Report 6, 45 pp.

Sverjensky, D. A. 1986. Genesis of Mississippi Valley-type lead–zinc deposits. Annual Review of Earth and Planetary Sciences, 14, 177–199.

Taylor, G.J., Wilmhurst, J.R., Togashi, Y. & Andrew, A.S., 1984. Geochemical and mineralogical halos about the Elura Zn–Pb–As orebody, western New South Wales. Journal of Geochemical Exploration, 22, 265–290.

Thompson, I.R., 1969. Summary of information on the Great Cobar Mine. Cobar Mines Proprietry Ltd. Internal report (unpublished).

Thomson, B.P., 1953. Geology and ore occurrence in the Cobar district. In: Edwards, A.B. (editor), Geology of Australian ore deposits. 5th Empire Mining and Metallurgical Congress, Melbourne. 863–896.

Tonkin, C., Clark, D.A. & Emerson, D.W., 1988. The magnetisation of the Elura orebody, Cobar, NSW. Exploration Geophysics, 19, 368–370.

Zaw, K, Huston, D.L., Large, R.R., Mernagh, T.P. & Ryan, C.G., 1994. Geothermometry and compositional variation of fluid inclusions from the Tennant Creek gold–copper deposits, Northern Territory: implications for exploration of auriferous ironstones. In: Hallenstein, C.P. (editor), Australasian Institute of Mining and Metallurgy, Annual Conference, Australian mining looks north; the challenges and choices. Australasian Institute of Mining and Metallurgy, Publication Series, 5/94, 185–188.

Received 28 July 1998; accepted 28 October 1998